



HAL
open science

GEMAS: Geochemical distribution of Mg in agricultural soil of Europe

Philippe Négrel, Anna Ladenberger, Clemens Reimann, Manfred Birke, Alecos Demetriades, Martiya Sadeghi, S. Albanese, M. Andersson, R. Baritz, M.J. Batista, et al.

► To cite this version:

Philippe Négrel, Anna Ladenberger, Clemens Reimann, Manfred Birke, Alecos Demetriades, et al.. GEMAS: Geochemical distribution of Mg in agricultural soil of Europe. *Journal of Geochemical Exploration*, 2021, 221, pp.106706 -. 10.1016/j.gexplo.2020.106706 . hal-03492808

HAL Id: hal-03492808

<https://hal.science/hal-03492808>

Submitted on 2 Jan 2023

HAL is a multi-disciplinary open access archive for the deposit and dissemination of scientific research documents, whether they are published or not. The documents may come from teaching and research institutions in France or abroad, or from public or private research centers.

L'archive ouverte pluridisciplinaire **HAL**, est destinée au dépôt et à la diffusion de documents scientifiques de niveau recherche, publiés ou non, émanant des établissements d'enseignement et de recherche français ou étrangers, des laboratoires publics ou privés.



Distributed under a Creative Commons Attribution - NonCommercial 4.0 International License

GEMAS: Geochemical distribution of Mg in agricultural soil of Europe

Philippe NÉGREL^{1,‡}, Anna LADENBERGER², Clemens REIMANN^{3,§}, Manfred BIRKE⁴, Alecos DEMETRIADES^{5,§}, Martiya SADEGHI² and the GEMAS Project Team⁶

¹ BRGM, Orléans, France, p.negrel@brgm.fr

² Geological Survey of Sweden, Uppsala, Sweden, anna.ladenberger@sgu.se, martiya.sadeghi@sgu.se

³ Geological Survey of Norway, Trondheim, Norway, clemensreimann@yahoo.co.uk

⁴ Bundesanstalt für Geowissenschaften und Rohstoffe, Stillweg 2, 30655 Hannover, Germany, Manfred.Birke@bgr.de

⁵ Institute of Geology and Mineral Exploration (IGME), 1 Spirou Louis St., Olympic Village, Acharnae, 13677 Athens, Hellenic Republic, alecos.demetriades@gmail.com

⁶ *The GEMAS Project Team*: S. Albanese, M. Andersson, R. Baritz, M.J. Batista, A. Bel-lan, D. Cicchella, B. De Vivo, W. De Vos, E. Dinelli, M. Đuriš, A. Dusza-Dobek, M. Eklund, V. Ernstsén, P. Filzmoser, B. Flem, D.M.A. Flight, S. Forrester, M. Fuchs, U. Fügedi, A. Gilucis, M. Gosar, V. Gregorauskiene, W. De Groot, A. Gulan, J. Halamić, E. Haslinger, P. Hayoz, R. Hoffmann, J. Hoogewerff, H. Hrvatovic, S. Husnjak, L. Janik, G. Jordan, M. Kaminari, J. Kirby, J. Kivisilla, V. Klos, F. Krone, P. Kwećko, L. Kutu, A. Lima, J. Locutura, D. P. Lucivjansky, A. Mann, D. Mackovych, J., Matschullat, M. McLaughlin, B.I. Malyuk, R. Maquil, R.G. Meuli, G. Mol, P. O'Connor, R. K. Oorts, R.T. Ottesen, A. Pasiieczna, W. Petersell, S. Pfeleiderer, M. Poňavić, S. Pramuka, C. Prazeres, U. Rauch, S. Radusinović, I. Salpeteur, R. Scanlon, A. Schedl, A.J. Scheib, I. Schoeters, P. Šeřčik, E. Sellersjö, F. Skopljak, I. Slaninka, A. Šorša, R. Srvkota, T. Stafilov, T. Tarvainen, V. Trendavilov, P. Valera, V. Verougstraete, D. Vidojević, A. Zissimos and Z. Zomeni.

[‡]Corresponding author

[§] Presently retired

30 **Abstract**

31
32 Agricultural soil (Ap-horizon, 0–20 cm) samples were collected from 33 European countries
33 as part of the GEMAS (GEOchemical Mapping of Agricultural and grazing land Soil) soil-
34 mapping project. The Mg data derived from total concentrations (XRF) and two acid
35 digestion methods, *aqua regia* (AR) and Mobile Metal Ion (MMI[®]), were used to provide an
36 overview of its spatial distribution in soil at the continental-scale. Magnesium is one of the
37 most abundant elements in the Earth's crust and essential nutrient for plants and animals and
38 its presence in soil is, therefore, important for soil quality evaluation.

39 In this study, the geochemical behaviour of Mg in European agricultural soil was investigated
40 in relation to a variety of soil parent materials, climatic zones, and landscapes. The chemical
41 composition of soil reflects mostly the primary mineralogy of the source bedrock, and the
42 superimposed effects of pre- and post-depositional chemical weathering, controlled by
43 element mobility and formation of secondary phases such as clays.

44 Low Mg concentrations in agricultural soil occur in regions with quartz-rich glacial sediments
45 (Poland, Baltic States, N. Germany), and in soil developed on quartz-rich sandstone parent
46 materials (e.g., central Sweden). High Mg concentrations occur in soil developed over mafic
47 lithologies such as ophiolite belts and in carbonate-rich regions, including karst areas. The
48 maximum extent of the last glaciation is well defined by a Mg concentration break, which is
49 marked by low Mg concentrations in Fennoscandia and north-central Europe, and high Mg
50 concentrations in Mediterranean region. Lithology of parent materials seems to play a key
51 role in the Mg nutritional status of agricultural soil at the European scale. Influence from
52 agricultural practice and use of fertilisers appears to be subordinate.

53 Comparison of the continental-scale spatial distribution of Mg in agricultural soil by using the
54 results from three analytical methods (XRF, AR and MMI[®]) provides complementary
55 information about Mg mobility and its residence time in soil. Thus, allowing evaluation of
56 soil weathering grade and impact of land use exploitation.

57

58 **Keywords:** weathering, parent materials, mineralogy, total concentration, partial extraction

59

60 **1 – Introduction**

61 In total, 2108 samples of agricultural soil (Ap-horizon, 0–20 cm) were collected from 33
62 European countries (5.6 million km²) as part of the GEMAS (GEOchemical Mapping of
63 Agricultural and grazing land Soil) project (Reimann *et al.*, 2014a, b). The study area covers
64 diverse groups of soil parent materials with a variable geological history, a wide range of
65 climate zones, and many different landscapes. The chemical composition of soil is mostly
66 controlled by the primary mineralogy of the source bedrock, the superimposed effects of the
67 last glaciation, pre- and post-depositional chemical weathering, formation of secondary
68 products such as clays, and element mobility (Négre *et al.*, 2015). All these factors contribute
69 to the geographical variation in the continental-scale spatial distribution of elements (Reimann
70 *et al.*, 2014c; Ladenberger *et al.*, 2015).

71 Magnesium is the eighth most abundant element in the upper continental crust (UCC)
72 of the Earth, with an average elemental abundance of 14 955 mg/kg (Rudnick and Gao, 2003).
73 Magnesium bearing minerals such as amphibole and pyroxene are common in mafic and
74 ultramafic rocks, e.g., basalt and gabbro. In sedimentary rocks, the main Mg bearing minerals
75 are carbonates, i.e., dolomite and magnesite. Magnesium is essential for all living organisms
76 and is not toxic under normal circumstances. It is a key plant nutrient and essential for
77 photosynthesis. It is used in industry (automotive, aircraft, train, laptop, mobile telephone,
78 tablet), steel, titanium and zirconium production, pharmaceutical and agricultural chemical
79 industries, and medical implants (Christie and Brathwaite, 2008). Magnesium may also be a
80 preferred material in all light-weight vehicles, hydrogen storage and advanced battery
81 technology. Currently, it is an essential alloying element in the aluminium industry.
82 Magnesium may be recovered from various resources, such as dolomite and Mg-bearing
83 evaporite minerals, Mg-bearing brines, and seawater (Christie and Brathwaite, 2008). All
84 these resources are globally widespread and estimated to constitute billions of tonnes of Mg.

85 Thus, Mg resources are considered as enormous and unlimited. Magnesium's current
86 criticality (i.e., economic importance versus supply risk; [European Commission, 2017](#)) is not
87 based on lack of Mg raw materials in Europe, but rather on trade issues as the worldwide
88 primary Mg production (around 878 Kt in 2016) is mainly supplied by China. However, the
89 development of research and development technologies will increase the long-term demand
90 worldwide.

91 Knowledge of the geochemical behaviour of this major element in the rock-soil cycle
92 through weathering processes is important, both for recognising soil nutritional status and for
93 targeting new Mg deposits. The GEMAS data set provides European-scale results for
94 chemical elements ([Reimann et al., 2014a, b](#)), including several so-called high-tech materials,
95 which are listed in the Critical Raw Materials list by the European Commission in 2017
96 ([Scheib et al., 2012](#); [Ladenberger et al., 2015](#); [Négre et al., 2016, 2019](#)). In this study,
97 geochemical data from the GEMAS project are used to (i) decipher the geochemical
98 behaviour of Mg using low-sampling density geochemical mapping at the continental-scale,
99 (ii) identify enriched and depleted regions of Mg, and (iii) interpret the Mg geochemical
100 patterns to highlight the respective impacts of soil weathering stage and land use in relation to
101 the different methods of analysis used, e.g., total analysis by X-ray Fluorescence (XRF),
102 strong acid extraction by *aqua regia*, and weak extraction by MMI[®].

103 **2 - General setting**

104
105 The GEMAS project ([Reimann et al., 2014a, b](#)) was carried out by the Geochemistry Expert
106 Group of EuroGeoSurveys with funding by national Geological Surveys, collaborating
107 Universities and Eurometaux (European Association of Metals). The project was managed by
108 the Geological Survey of Norway. Soil samples from two land-use types (agricultural soil ,
109 n=2108; grazing land soil, n=2024) were collected in 33 European countries, covering an area

110 of about 5.6 million km² with an average density of 1 sample/2500 km² (Reimann et al.,
111 2012a; 2014a, b). The countries covered are shown in Figure 1. The main objective of the
112 pan-European project was to map the element variation in agricultural and grazing land soil,
113 and to assess the impact of agricultural activities. Soil samples were not collected at known
114 contaminated sites, in the immediate vicinity of industrial sites, power plants, railway lines,
115 major roads, directly below high-power electric lines and near to pylons. The GEMAS *aqua*
116 *regia* and XRF results were provided in a two-volume geochemical atlas (Reimann et al.,
117 2014a, b), followed by a series of peer-review publications where detailed interpretation of
118 the continental-scale distribution of single elements or related groups of elements or physical
119 parameters of soil were presented, e.g., Reimann et al. (2012a; Pb), Ottesen et al. (2013; Hg),
120 Tarvainen et al. (2013; As), Scheib et al. (2012; Nb), Sadeghi et al. (2013; Ce, La, Y),
121 Ladenberger et al. (2015; In), Albanese et al. (2015; Cr, Ni, Co, Cu), Négrel et al. (2016,
122 2018a, b, 2019; - Ge, U-Th, Rb-Ga-Cs, Sc-W-Li), Fabian et al. (2014; pH), Birke et al. (2016,
123 2017; Cd), Jordan et al. (2018; Ni), Matschullat et al. (2018; C-N-S), Hoogewerff et al. (2019;
124 Sr), Xu et al. (2019; pH, C).

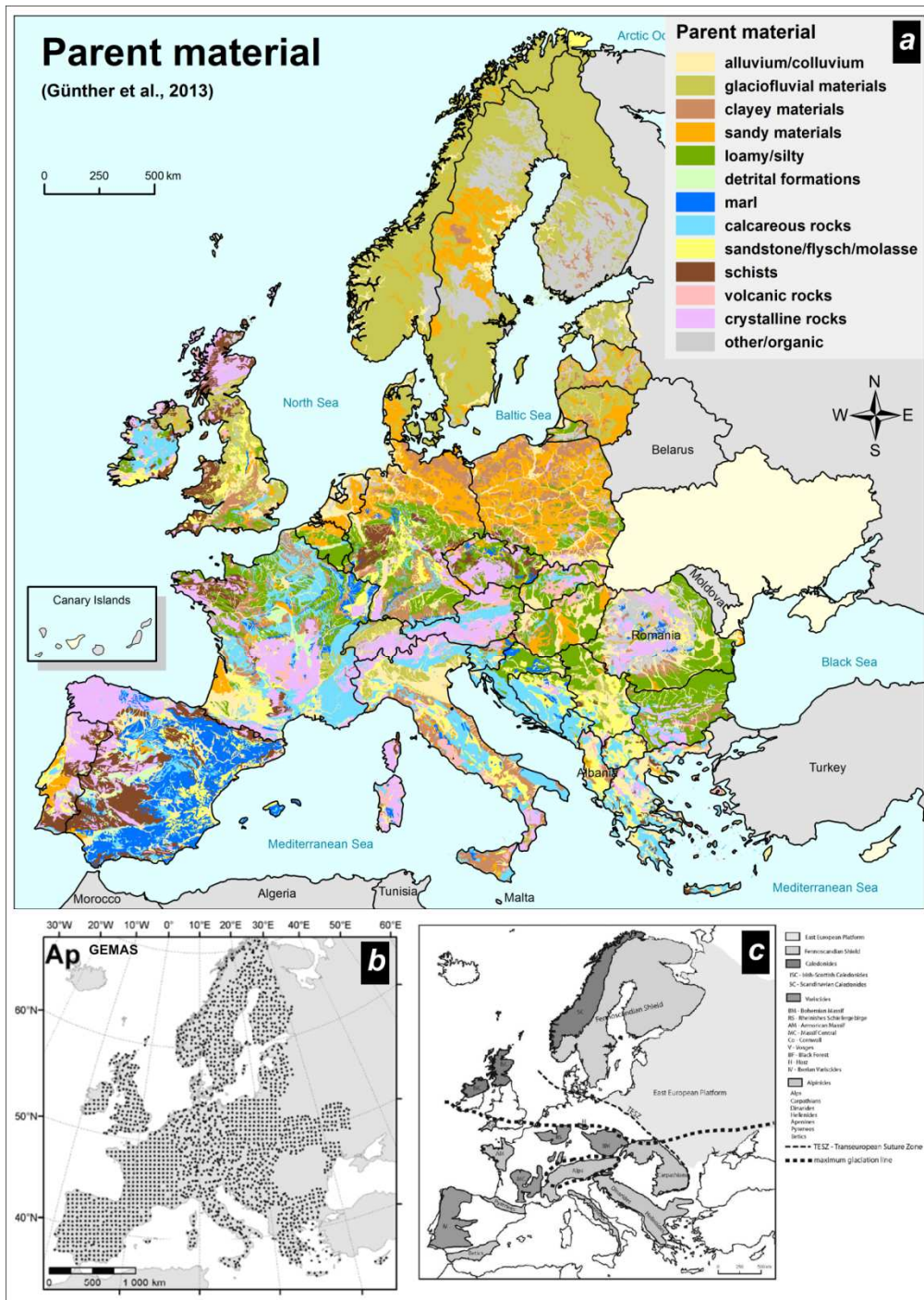
125 **3 – Material and methods**

126 **3.1. Sampling and sample preparation**

127 Two land use soil types were collected from agricultural and grazing land, with a nominal
128 sampling density of 1 sample per 2500 km² (Fig. 1b). Grazing land soil (Gr) was defined as
129 ‘land under permanent grass cover’ and the sampling depth range was 0–10 cm according to
130 REACH (Registration, Evaluation, Authorisation, and Restriction of Chemicals) regulation
131 requirements (REACH, 2006). The agricultural soil (Ap) was collected from the ploughing
132 layer of an arable field at a depth range of 0–20 cm, again according to REACH regulations.
133 Each agricultural or grazing land soil sample (*ca.* 3.5 kg) corresponds to a composite of five
134 sub-samples, taken from the corners and centre of a 10 × 10 m square. The total number of Ap

135 samples is 2108 and that of Gr 2024 samples. All soil samples for analysis and storage were
136 prepared in a single facility (State Geological Institute of Dionyz Stur, Slovakia). Sample
137 preparation involved air-drying at ambient temperature, sieving to <2 mm using a nylon
138 screen, homogenising, and final splitting into 10 sub-samples ([Mackovych and Lucivjansky,](#)
139 [2014](#)). The analytical results for Ap and Gr samples are, with very few exceptions, highly
140 comparable and, thus, the latter are not being further discussed in this study.

141



142

143 *Figure 1. Modified from Négrel et al. (2015, Fig. 1, p.3). (a) Map of soil parent materials in Europe*
 144 *showing the distribution of various lithologies across the continent (modified from Günther et al.,*
 145 *2013 and adapted from Négrel et al., 2015, Fig. 1, p.3). (b) Sample locations of the ploughed*
 146 *agricultural soil sample sites (dots); (Ap-samples, n=2108). Map projection: ETRS89 Lambert*
 147 *Azimuthal Equal-Area projection coordinate reference system, with central meridian at 10°. (c)*
 148 *Generalised geotectonic map of Europe with major lithotectonic units, Variscan and Alpine belts,*
 149 *Trans-European Suture Zone (TESZ) and the extension of maximum glaciation (modified from*
 150 *Reimann et al., 2012a, Fig. 1, p.198).*

151 **3.2. Chemical analysis and quality control**

152 The GEMAS project soil samples were analysed using total and partial extraction methods
153 (for details refer to: [Reimann et al., 2009, 2011, 2012b](#); [Birke et al., 2014a](#)). Two project
154 reference materials, prepared in the same laboratory (State Geological Institute of Dionyz
155 Stur, Slovakia), were used to monitor analytical performance ([Demetriades et al., 2014](#);
156 [Reimann and Kriete, 2014](#)).

157 Total concentrations of Mg were determined by XRF, and 7% of the results are below
158 the detection limit of 302 mg/kg. In addition, two partial extractions were used, as described
159 below.

160 Hot *aqua regia* digestion, representing a strong partial extraction and recommended in
161 environmental and agricultural soil studies (e.g., [Vercoutere et al., 1995](#); [Santos and Alleoni,](#)
162 [2013](#); [Sastre et al., 2002](#)), was applied on the collected soil samples. It is stressed that residual
163 elements not released by *aqua regia* digestion are mostly bound to silicate minerals, and are
164 considered unimportant for estimating the mobility and behaviour of elements ([Niskavaara et](#)
165 [al., 1997](#); [Chen and Ma, 2001](#)).

166 A soil sample weight of 15 g of the <2 mm fraction was leached in 90 ml *aqua regia*
167 (95°C, 1 hour), and then made-up to a final volume of 300 ml with 5% HCl. The supernatant
168 solutions of over 5000 soil samples were analysed for 53 elements using a combination of
169 Inductively Coupled Plasma Mass Spectrometry (ICP-AES) and Atomic Emission
170 Spectrometry (ICP-MS) (ACME Laboratories in Vancouver, Canada; now Bureau Veritas
171 Mineral Laboratories). Quality control was monitored using field duplicate-replicate splits,
172 and matrix matched standards and reference materials. Only 5% of the agricultural soil
173 samples have Mg concentrations below the detection limit of 50 mg/kg. The hot *aqua regia*
174 digestion is able to extract elements adsorbed on clay minerals, dissolved Fe and Mn oxides
175 and carbonate minerals, and can even dissolve some silicate phases (e.g., olivine, biotite,

176 pyroxene), while other silicates and oxides are only weakly to moderately dissolved (Dolezal
177 et al. 1968; Räsänen et al., 1992; Aatos et al., 1994; Snäll and Liljefors, 2000; Vilà and
178 Martínez-Lladó, 2015). Comparison of the *aqua regia* with the XRF data often provides an
179 insight to the host mineralogy for the element(s) being studied.

180 The Mobile Metal Ion (MMI[®]) method is a weak partial extraction technique
181 originally developed for mineral exploration (Mann et al., 1998), and was applied on the
182 agricultural soil samples (Ap) with the purpose of identifying those weakly adsorbed elements
183 that are bioavailable and may also be related to weathering processes and anthropogenic
184 factors (Mann et al., 2015; Sadeghi et al., 2015). The MMI[®] method, based on having a
185 number of strong ligands in a neutral to alkaline-buffered solution (Mann, 2010; Mann et al.,
186 2014a), enables ions that are weakly adsorbed onto soil particle surfaces to be brought into
187 solution for determination by ICP-MS (Mann et al., 2014b). This analytical method allows,
188 therefore, the evaluation of those elements that are mobile, and potentially bioavailable in soil
189 (e.g., Reimann et al., 2012a). The MMI[®] analytical method is a proprietary technique that
190 uses a high sample to solution ratio and a weak solution (MMI[®]-M) to extract only the more
191 accessible, or mobile metal ions. The Ap samples were analysed by MMI[®] extraction using a
192 50-g sample weight, which was shaken for 30 minutes in 50 ml of MMI[®]-M solution before
193 being centrifuged and the resultant leachate analysed by ICP-MS for 57 elements at SGS
194 Mineral Services in Toronto, Canada. Around 19% of the Ap samples have Mg concentrations
195 below the detection limit of 1 mg/kg.

196 A rigorous quality control (QC) procedure was part of the sampling and analytical
197 protocols of the GEMAS project (Reimann et al., 2009, 2011, 2012b; Demetriades et al.,
198 2014). The agricultural and grazing land soil samples were analysed in batches of twenty. In
199 each analytical batch were included one field duplicate, one analytical replicate of the field
200 duplicate and the project standard. An innovation of the GEMAS project was the calculation

201 of the practical detection limit (DL) of each determinand using the results of the project
202 replicate samples through the estimation of regression line coefficients by the ‘reduced major
203 axis line’ procedure (Demetriades, 2011). A detailed description of the analytical methods and
204 quality control procedures are provided in the GEMAS project atlas (Birke et al., 2014a;
205 Reimann and Kriete, 2014; Demetriades et al., 2014), and in three technical reports (Reimann
206 et al., 2009, 2011, 2012b). Quality control procedures for the MMI[®] extraction method for the
207 entire Ap data set are described in Reimann et al. (2012b) and Mann et al. (2014a, b). Only
208 the data obtained for the Ap soil samples will be considered hereafter.

209 **3.3 Data treatment**

210 Geochemical data are a classical example of compositional data, element
211 concentrations reported in wt % or mg/kg sum up to a constant and are thus not free to vary.
212 The information value of such data generally lies in the ratios between the variables (Beus and
213 Grigorian, 1977; Reimann et al., 2012a). Compositional data do not plot in classical Euclidean
214 space, but they have their own geometry, the Aitchison simplex (Aitchison, 1986; Buccianti et
215 al., 2006; Pawlowsky-Glahn and Buccianti, 2011). Thus, only order statistics should be used
216 in the processing of geochemical data, noting that percentiles are unchanged under log-
217 transformation. This is not the case, however, under a log-ratio-transformation.

218 The coloured surface map of each determinand was produced by kriging, based on a
219 careful variogram analysis (Filzmoser et al., 2014). Kriging was used to interpolate values of
220 each determinand from the irregularly distributed sampling sites to a regular grid and into
221 unsampled space. Comparison with black and white point source maps has shown that the
222 kriged maps reflect the spatial structure of the data very well (Reimann et al., 2014c). Class
223 limits, used for the colour maps are based on percentiles (5, 25, 50, 75, 90 and 95). Maps
224 displayed hereafter (Figs. 7-9) were produced in Esri’s ArcGIS software.

225 Ten geological parent material subgroups were constructed for processing the Ap soil
 226 data set (Birke et al., 2014b): (1) alk: alkaline rocks; (2) chalk: calcareous rocks; (3) granite:
 227 plutonic felsic rocks; (4) green: greenstone, basalt, mafic bedrocks; (5) loess: loess; (6) org:
 228 organic soil; (7) other: unclassified bedrocks; (8) prec: predominantly Precambrian bedrocks
 229 (granitic gneiss); (9) quartz: soil developed on coarse-grained sandy deposits (e.g., the end
 230 moraines of the last glaciation), and (10) schist: schist. In addition, the relative proportions of
 231 six major lithological types were recalculated for the GEMAS project area (Reimann et al.,
 232 2012c), based on the global rock lithology presented by Amiotte-Suchet et al. (2003). Among
 233 these major lithologies, plutonic and metamorphic rocks (39%) and shale (37%) dominate;
 234 carbonate rocks (14%) and sand-sandstone (9.5%) are significant, whereas felsic volcanic
 235 rocks and basalt (0.5% each) play a subordinate role.

236 4 – Results and Discussion

237 4.1 Mg concentrations in agricultural soil

238 The minimum, median and maximum concentrations of Mg delivered by the GEMAS project,
 239 using the three analytical methods (XRF, AR and MMI[®] extractions), are provided in Table 1
 240 together with the detection limit (DL) and percentage of samples under DL.

241

242

243

244

245

246 *Table 1. Basic statistical parameters for Mg in European agricultural (Ap) soil samples determined by different*
 247 *analytical methods.*

248

Method	N	DL mg/kg	%<DL	Minimum mg/kg	Median mg/kg	Maximum mg/kg
XRF	2108	302	7	<302	5488	126368
AR	2108	50	5	<50	2860	116908

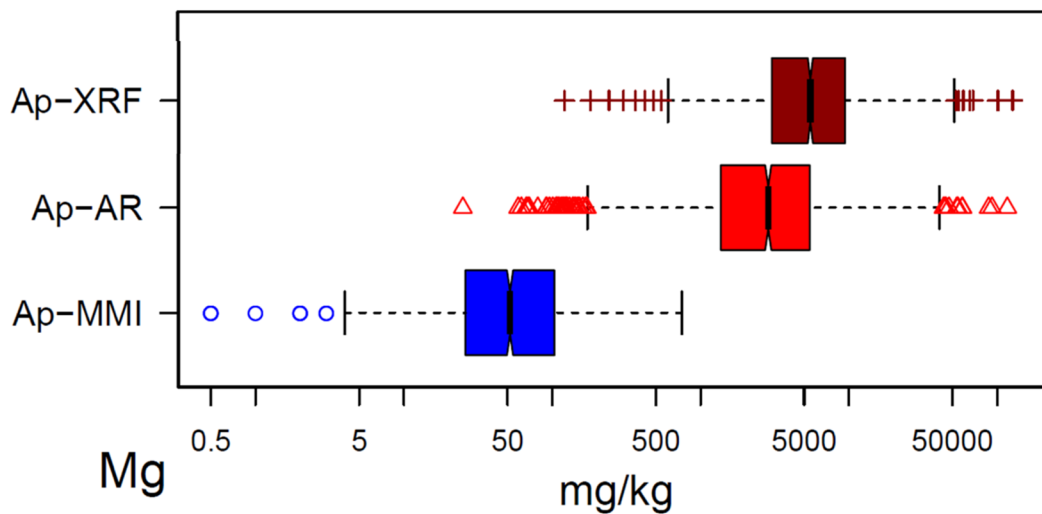
MMI	2108	1	19	<1	52	>500*
-----	------	---	----	----	----	-------

*upper detection limit of Mg in the MMI® extraction is 500 mg/kg

249

250 The boxplots comparing the Mg results of Ap soil samples clearly show the
 251 differences between the three analytical techniques (Fig. 2). They display a number of upper
 252 and lower outliers (only lower outliers for the MMI® data), which are, however, not far away
 253 from the main body of data (note the log-scale used). There is no significant overlap between
 254 the main body of the XRF, AR and MMI® data. The 95% confidence interval on the median,
 255 displayed by the notches, shows that there is no overlap, suggesting that there is a distinct
 256 difference at the 5% significance level among the Ap XRF, AR and MMI® data sets of Mg.

257



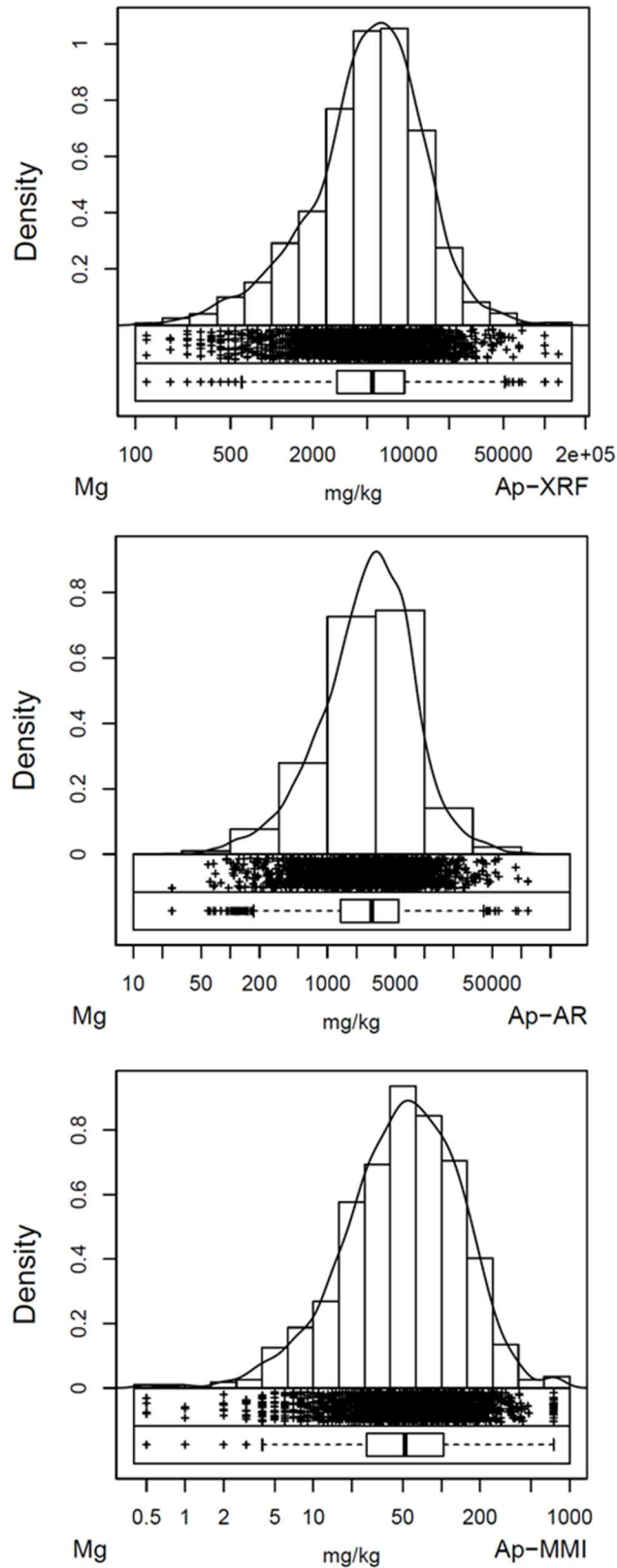
258

259 *Figure 2. Boxplot comparison of Mg concentrations in European Ap soil samples determined by XRF,*
 260 *aqua regia and MMI®. Refer to Table 1 for the basic statistical parameters.*

261

262 Compared to the UCC total Mg average (14,955 mg/kg) by [Rudnick and Gao \(2003\)](#),
 263 the median Mg concentration (5488 mg/kg), measured by XRF, is substantially lower in the
 264 European agricultural soil samples (ratio median Ap/UCC = 0.367). This may suggest a
 265 possible overestimation of the UCC Mg value in previous calculations, or it may also be an
 266 indication of an overall depletion/removal of this important plant nutrient in agricultural soil.

267 The combination plot histogram - density trace - one-dimensional scattergram - boxplot (Fig.
268 3) shows the Mg univariate data distribution. The one-dimensional scattergram and boxplot
269 highlight the existence of a substantial number of outliers in the Mg distribution. The density
270 trace and histogram are overall symmetrical in the log-scale.



271

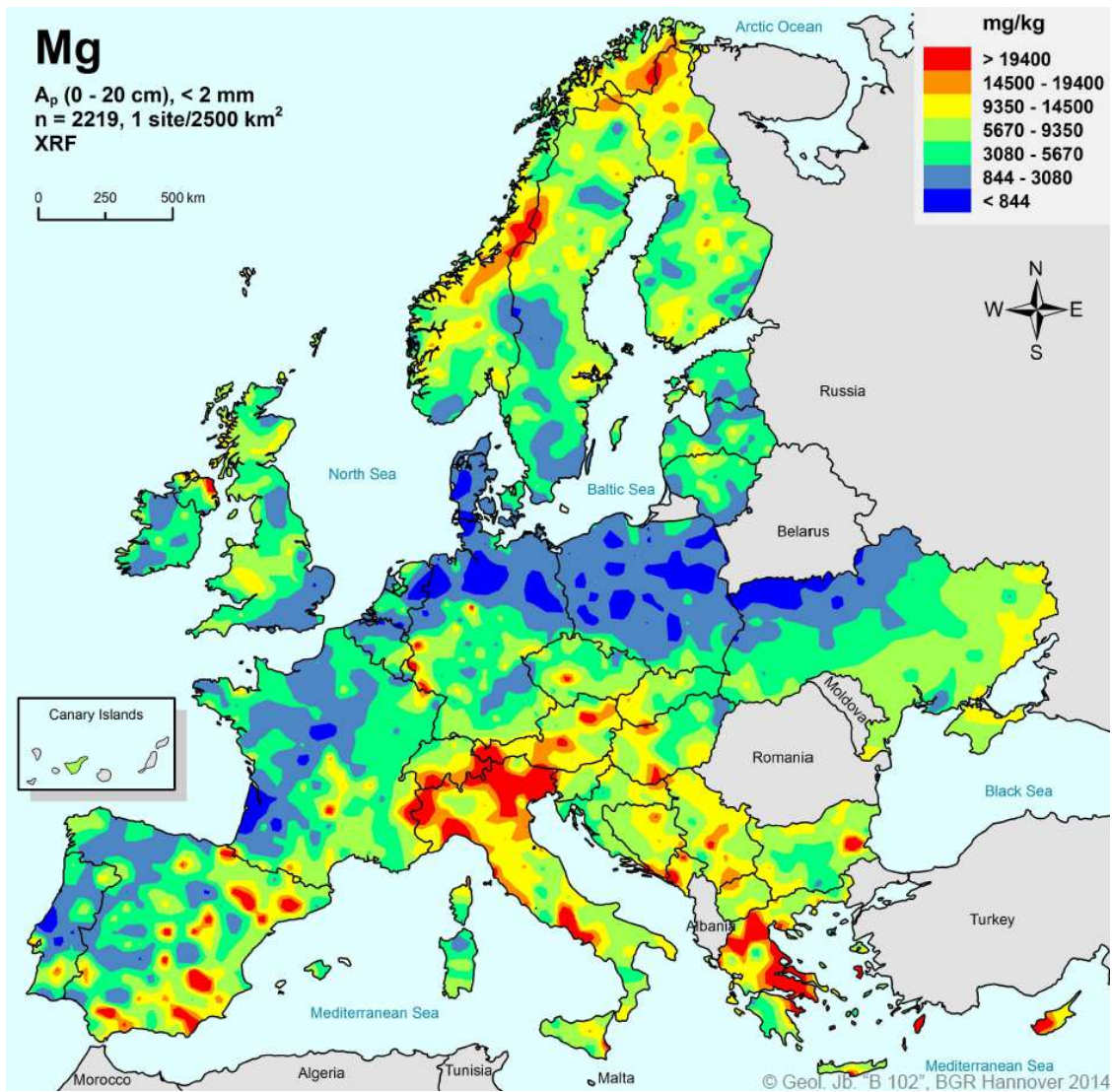
272 *Figure 3. Combination plot of histogram, density trace, one-dimensional scatter-diagram and boxplot*
 273 *of the Mg distribution in European Ap soil samples determined by XRF (a), and ICP-AES/MS after an*
 274 *aqua regia (b), and MMI[®] extraction (c). Note in the density trace the upper limit of 500 mg in the*
 275 *MMI[®] extraction.*

276 4.2 Spatial distribution of Mg in Ap soil

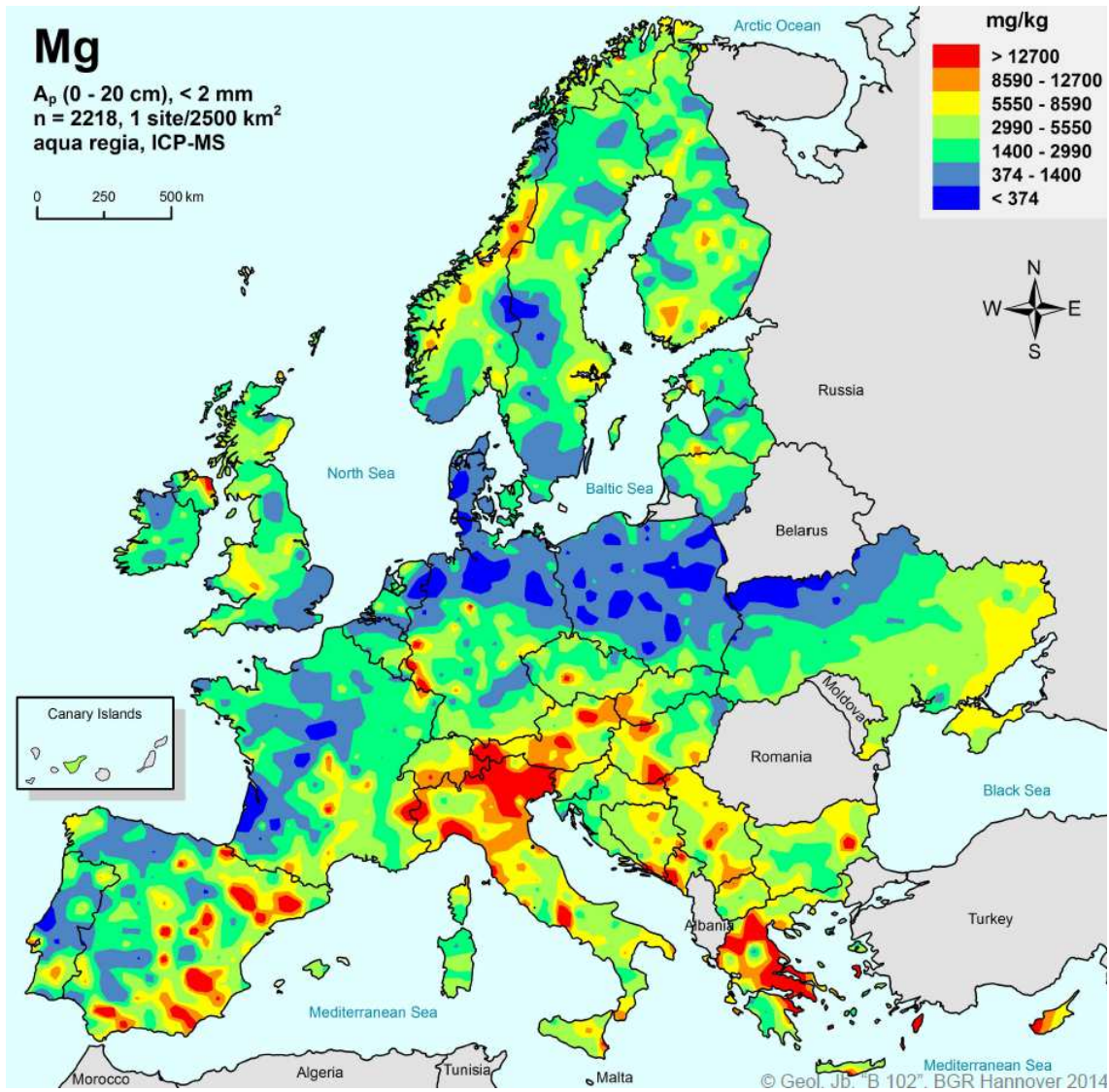
277 The maps of Mg determined by XRF, and ICP-AES/MS following *aqua regia* and MMI[®]
278 extractions are presented in Figures 6, 7 and 8. Although the map of total Mg concentrations
279 determined by XRF (Fig. 6) shows considerably higher concentrations (median 5488 mg/kg)
280 in soil than the map of *aqua regia* extraction (median 2860 mg/kg), with average Mg
281 extractability of 55% (Reimann et al., 2011), the overall continental-scale spatial distribution
282 is quite similar.

283 The two classical maps of Mg arising from the *aqua regia* extraction and XRF (Figs. 6
284 and 7) show unusually low Mg concentrations over the coarse-grained sediments of the last
285 glaciation in central-northern Europe. This is due to the mineralogical composition of these
286 glacial sands, which consist almost exclusively of quartz (SiO₂) (Zeeberg, 1998; Reimann et
287 al., 2012c; Scheib et al., 2014). The southern limit of the last glaciation is thus still visible as a
288 Mg concentration break on both maps. The median Mg concentrations between northern and
289 southern Europe are different by a factor of 2.4 (1500 vs. 3600 mg/kg, respectively), and are
290 not as contrasted as for many other elements determined on the GEMAS project soil samples
291 (Reimann et al., 2014c). For *aqua regia* extractable Mg concentrations in the agricultural soil
292 of European countries, the highest Mg median value is in Cyprus (8785 mg/kg), followed by
293 Montenegro (8098 mg/kg) and the Hellenic Republic (Hellas) (7845 mg/kg), countries with
294 known ophiolite complexes (mafic and ultramafic intrusions). The lowest median value
295 occurs in Poland (716 mg/kg); whereas, areas underlain by limestone (e.g., eastern and
296 southern Spain), dolomite (Alps) and mafic-ultramafic rocks (e.g., Hellas, Norway and
297 Finland) appear as large Mg anomalies on the map. Further, clay-rich soil such as the Central
298 Scandinavian Clay Belt (central Sweden) is also visible as a Mg anomaly on the maps
299 (Figures 6-8). One of the principal differences between XRF and AR geochemical maps is the
300 intensity difference of Mg anomalies in Fennoscandia, which may indicate the widespread

301 occurrence of yet unweathered Mg-silicates in northern Europe that do not dissolve in *aqua*
302 *regia*.



303
304 *Figure 6. Geochemical map for Mg total concentrations in ploughed agricultural soil (A_p, n=2108)*
305 *(XRF results). Interpolation by kriging, range = 1 000 km, and search radius = 300 km (from*
306 *Reimann et al., 2014c, Fig. 11.34.5, p.300).*
307



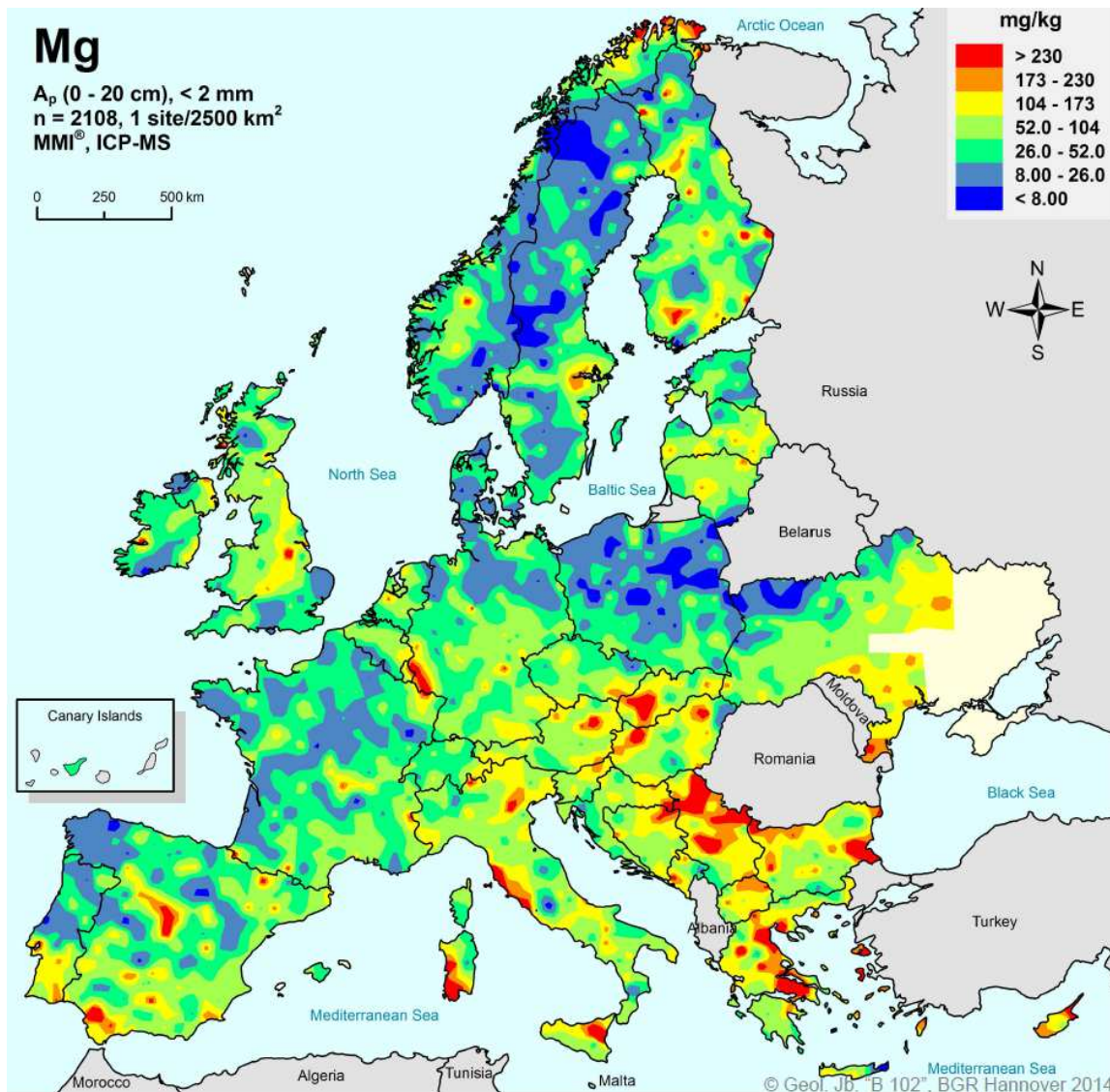
308

309

310 *Figure 7. Geochemical map for aqua regia extractable Mg concentrations in ploughed agricultural*
 311 *soil (A_p , $n=2108$). Interpolation by kriging, range = 1 000 km, and search radius = 300 km (from*
 312 *Reimann et al., 2014c, Fig. 11.34.5, p.299).*

313

314



315
 316

317 *Figure 8. Geochemical map for MMI[®] extractable Mg concentrations in ploughed agricultural soil*
 318 *(A_p , $n=2108$). Interpolation by kriging, range = 1 000 km, and search radius = 300 km (from*
 319 *Reimann et al., 2014a, Figure on accompanying DVD).*

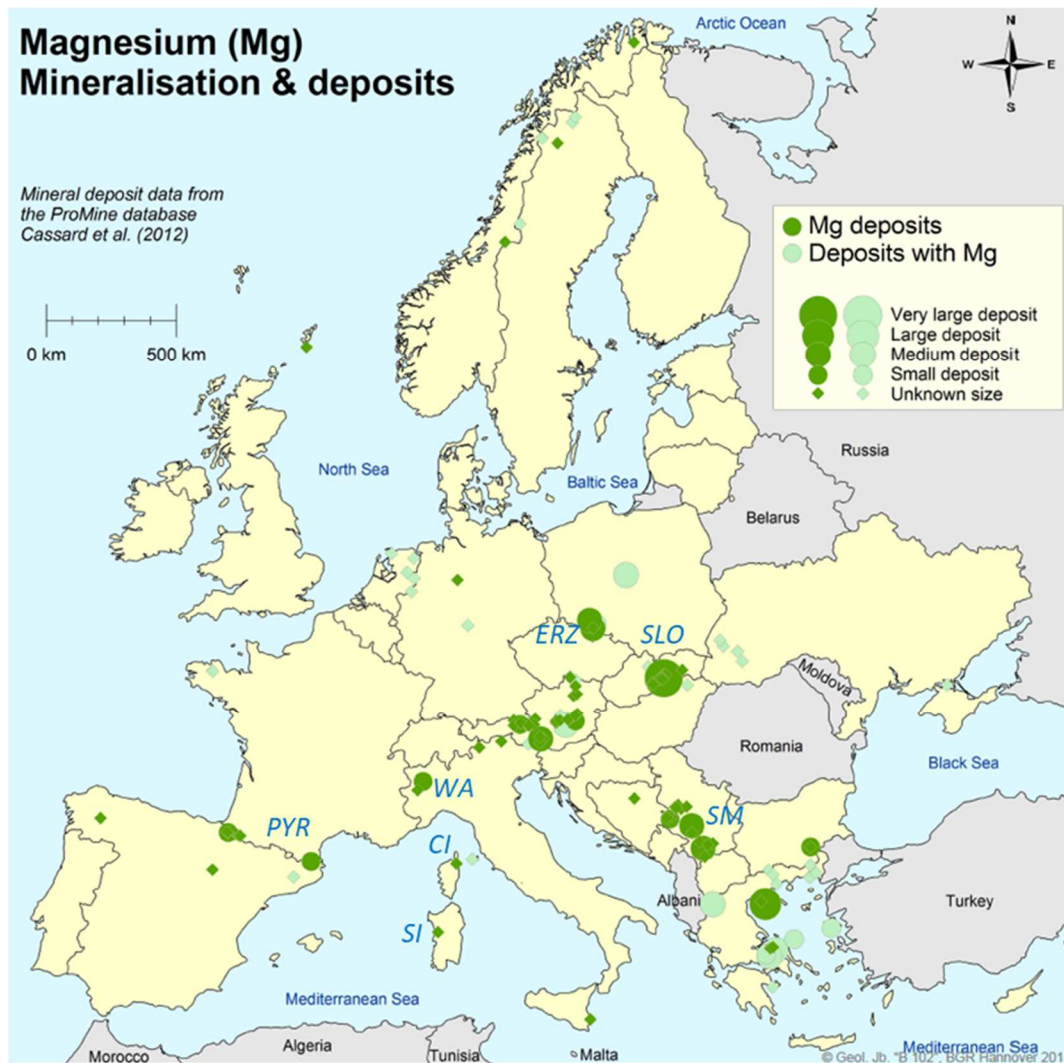
320
 321

322 The map of Mg results from MMI[®] extraction on A_p soil samples (Fig. 8) shows
 323 rather complementary pattern in comparison to both the *aqua regia* (Fig. 7) and XRF (Fig. 6)
 324 geochemical maps. The features shared by all three maps are: (1) the southern limit of the last
 325 glaciation; (2) the major Mg anomalies appear to be related to the occurrence of mafic-
 326 ultramafic rocks (intrusive and volcanic) and dolomite or dolomitic limestone; (3) regions
 327 with silica-rich loose sandy deposits and granitic bedrock are usually outlined by low Mg
 content in soil, and (4) low pH facilitating Mg removal from soil may contribute to low Mg

328 anomalies irrespectively of the underlying bedrock, e.g., in central Sweden, in northern-
329 central Europe and NW Spain. However, apart from many similarities, some interesting
330 differences can also be observed. In northern Fennoscandia, high Mg content in soil, caused
331 by Palaeoproterozoic greenstone belts and Caledonian mafic and ultramafic rocks, are well
332 outlined on the XRF Mg map. In comparison, on the *aqua regia* Mg map these features are
333 shown with a decreasing intensity to disappear completely on the MMI[®] map. There are
334 possibly two reasons for this geochemical behaviour of Mg; either Mg is hosted by resistant
335 silicate minerals which have a limited dissolution in these acids, or low soil pH effectively
336 removes weakly bound Mg from soil particles resulting in very low Mg content in acid
337 extractions. Another interesting example can be observed in Sardinia, where the Mg MMI[®]
338 map has a very contrasting pattern, with high concentrations in the south-western and low in
339 the north-eastern parts of the island, features that are not visible on either the XRF or AR
340 maps. In this case, the distinct contrast is most likely caused by a lithology difference, i.e.,
341 occurrence of a low Mg granite in the NE, and Mg enriched sedimentary rocks, especially
342 limestone and dolomite, in the SW.

343

344



345

346 *Figure 9. Distribution of Mg-bearing ore deposits in Europe (based on the ProMine Mineral*
 347 *Database; Cassard et al., 2012, 2015; Demetriades and Reimann, 2014). Abbreviations of*
 348 *mineralised districts: CI: Corsica Island; ERZ: Erzgebirge (Ore Mts.); PYR: Pyrenees; SI:*
 349 *Sardinia Island; SM: Serbo-Macedonian ore district; SLO: Slovakia; WA: Western Alps.*
 350

351 The geographical distribution of the Mg deposits in Europe is shown in Figure 9. Most
 352 important Mg mineral resources are hosted by ultramafic lithologies and their
 353 weathering/alteration products (magnesite), carbonate rocks (dolomite) and chemical deposits
 354 (carnallite) as given by Cassard et al. (2012, 2015). The classification of Mg deposits on the
 355 ProMine map (Figure 9) is based on threshold values for Mg in metric tonnes (t): class A for
 356 super-large deposits (100,000,000 t), class B for large deposits (10,000,000 t), class C for
 357 medium deposits (1,000,000 t), and class D for small deposits (100,000). Many of the
 358 magnesium deposits are represented by magnesite and contact metamorphic deposits of

359 brucite along granite-dolomite contacts. Magnesite in the Caledonides, Hellas and Italy are
360 associated with the ultramafic parts of ophiolites (Pohl, 1990). Magnesia can be also produced
361 from surface or subterranean brines (Christie and Brathwaite, 2008). Natural magnesite occurs
362 in few large, high grade (70-90% MgCO₃) and a large number of small, lower grade (>12%
363 MgCO₃) deposits either as crystalline or amorphous phases. Crystalline deposits of magnesite
364 occur in Austria and Spain, whereas amorphous magnesite deposits are known in Austria and
365 Hellas (Christie and Brathwaite, 2008). The correlation between the location of Mg deposits
366 and Mg anomalies in agricultural soil is relatively good, if a rather random distribution of Mg
367 deposits across the continent is considered. The XRF Mg anomalies correlate well with Mg
368 deposits in Central Caledonides (Sweden and Norway), northernmost Norway and Finland, in
369 Austria and in the Alps (Italy, Austria), Balkan region and Hellas, SE Sicily, N Corsica and N
370 Spain (Pyrenees and its foreland). *Aqua regia* extractable Mg anomalies largely follow XRF
371 results (due to relatively high Mg extractability). The MMI[®] Mg results in agricultural soil
372 display additional anomalies, which follow ProMine Mg deposits in SW Sardinia and
373 Hellenic island of Lesbos in the eastern Aegean Sea. In contrast to XRF and AR data, MMI[®]
374 results do not show high Mg concentrations in Central Caledonides of Norway and Sweden.
375 This phenomenon can be related to climate, dry conditions with low precipitation in an
376 environment with presumable alkaline soil (>7 pH) in the Mediterranean region, and high
377 precipitation combined with acidic soil (<6 pH) and rapid wash-out in the mountain region of
378 the Scandinavian Caledonides.

379

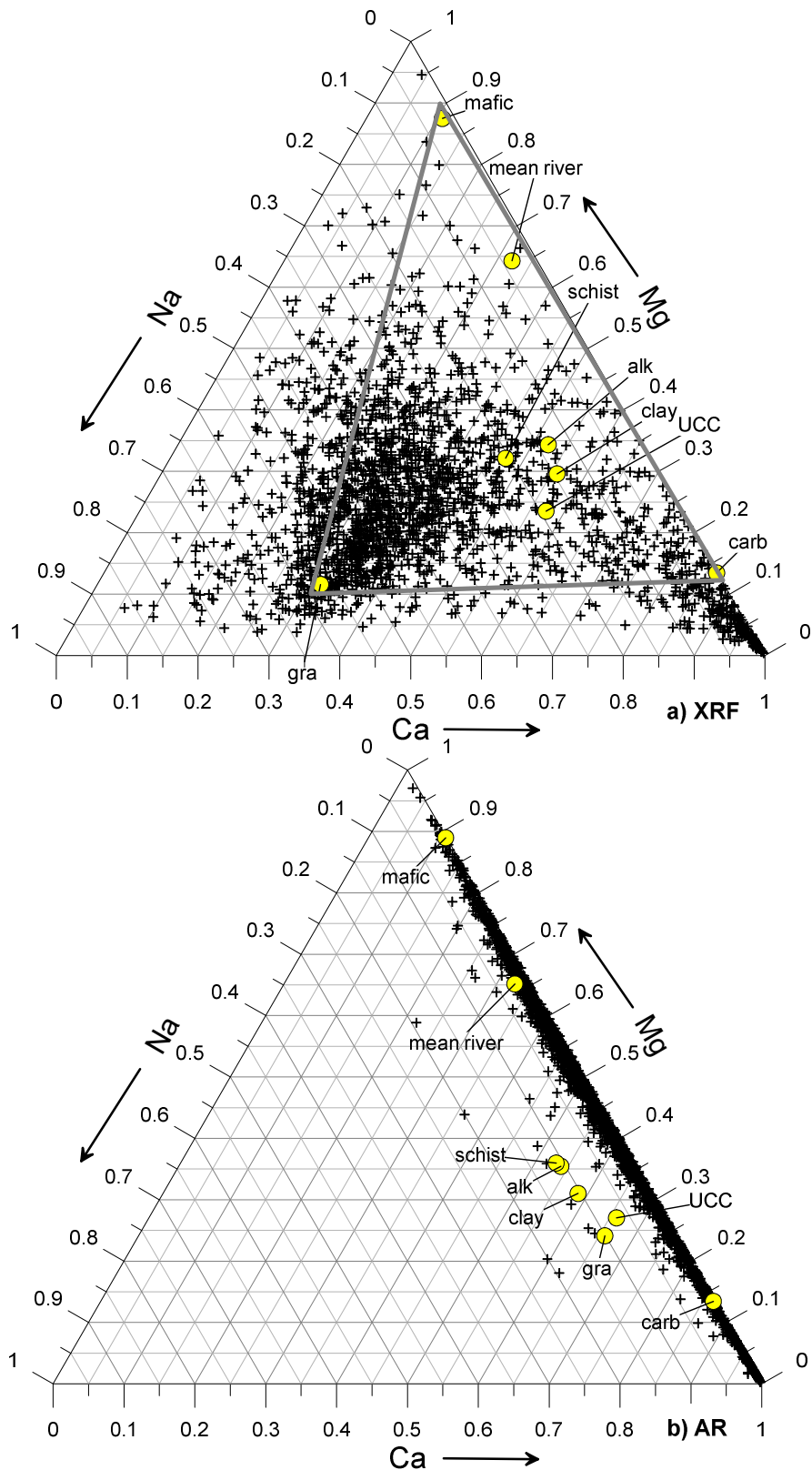
380 **4.3. The role of parent material on Mg variation in soil at the European scale**

381 The chemical composition of sediments and soil represents, to a large extent, the primary
382 mineralogy of the source bedrock, the effects of pre- and post-depositional chemical
383 weathering, formation of secondary products such as clays, and element mobility, either by
384 leaching or mineral sorting with superimposed effects of glaciation. Therefore, Mg in soil,

385 like Al and K, is often retained in weathering soil profiles, compared to Na and Ca, which are
386 rapidly leached as dissolved ions. Liming and use of Mg fertilisers are the main anthropogenic
387 interferences on natural Mg-cycles.

388 To evaluate the input from parent materials and chemical weathering trends, ternary
389 plots of carefully selected parameters can be used (e.g., [Kasanju et al., 2008](#); [Négre et al.,](#)
390 [2015](#)). Comparison of Ca, Na and Mg total XRF and AR contents in Ap soil samples (Fig.
391 10a and b) allows discrimination between carbonate and silicate parent materials including
392 various siliciclastic components (low Ca granite, sandstone and ultramafic rocks). XRF results
393 (Fig. 10a) show that soil chemical composition is scattered between three extreme end-
394 members, defined by mafic-ultramafic rocks, carbonates (limestone) and low Ca granite
395 variation. The carbonate-rich soil forms a distinct group on the diagram, while soil developed
396 on silicate parent materials has a rather large spread with predominance of felsic source rocks
397 (towards low Mg composition), and deviates from typical UCC end-members (Fig. 10a).

398 The *aqua regia* results of Ca-Mg-Na in Figure 10b show a trend dominated by the
399 correlation between Mg and Ca, while Na is exceptionally low. This pattern might be simply
400 the result of a difference between extractability of Ca, Mg and Na, with the first two being
401 highly soluble in AR, while Na has low extractability. This would indicate that the pattern is
402 not related to the type of source parent materials.



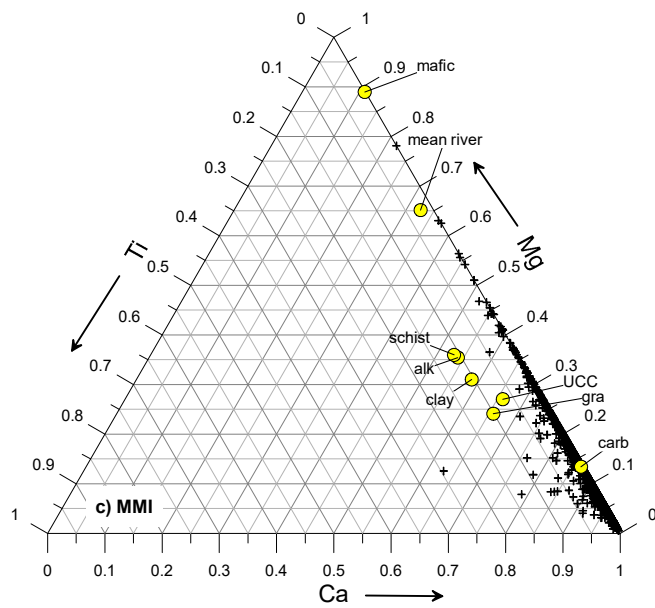
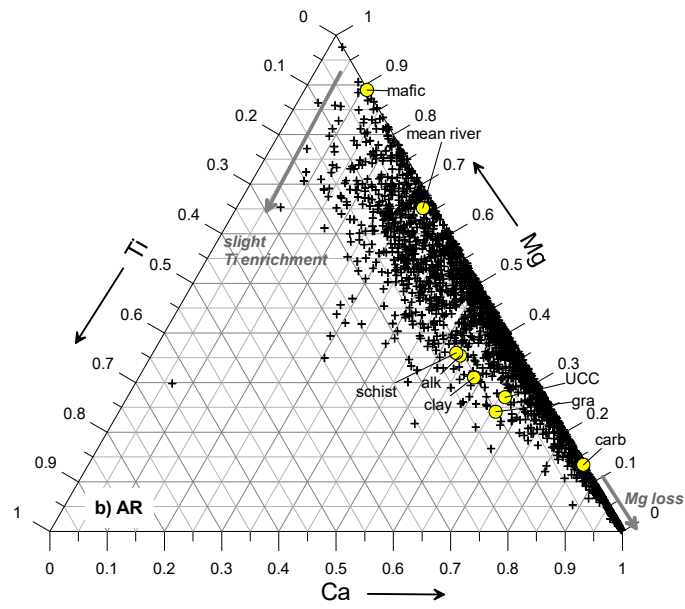
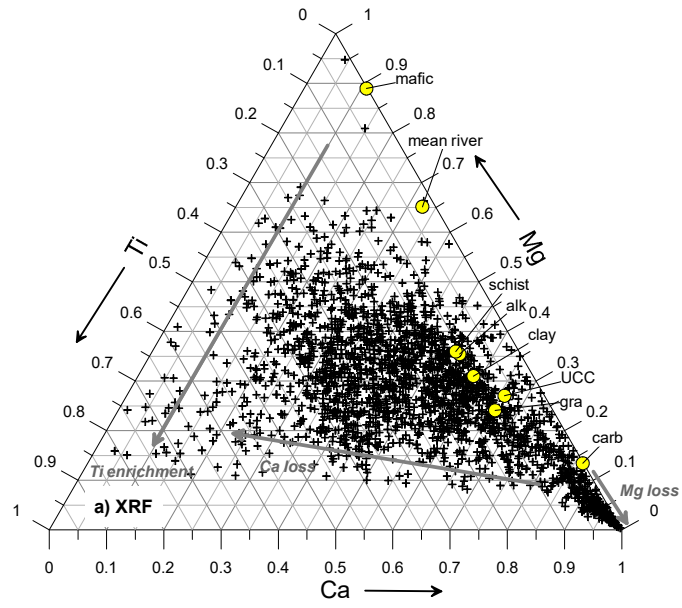
403

404 *Figure 10. Ca–Mg–Na (in molecular proportions) distribution in GEMAS agricultural soil samples*
 405 *(black crosses), plotted together with bedrock and Upper Continental Crust (UCC) composition*
 406 *(yellow circles) according to Parker (1967) and Rudnick and Gao (2003), respectively. Calcium, Mg*
 407 *and Na Ap data from (a) XRF and (b) aqua regia.*

408 A second ternary plot is the Ca, Mg and Ti association (Figure 11), using their
409 contents in molecular proportions in the GEMAS Ap samples of the XRF (Fig. 11a) *aqua*
410 *regia* (Fig. 11b) and MMI[®] (Fig. 11c) results. The GEMAS Ca, Mg and Ti Ap data are plotted
411 together with the main lithological end-members taken from [Parker \(1967\)](#), e.g., plutonic and
412 metamorphic rocks and shale, carbonate rocks and sand-sandstone, and the upper continental
413 crust average from [Rudnick and Gao \(2003\)](#). Using Ti as an insoluble element allows
414 discrimination compared to more soluble elements during weathering like Ca and Mg.

415 In Figure 11a representing the XRF total concentrations, the main spread of data along
416 the Mg axis reflects the variation in Mg content between sedimentary end-member (carbonate
417 and sandstone) and mafic (ultramafic rocks) end-member parent materials. The closeness of a
418 soil sample approaching the 10% apex along the Mg axis is an indication of similarity to a
419 lithological end-member, with additionally Mg loss during carbonate weathering. The
420 arrowhead lines denote compositional trends of weathering of silicate and carbonate rock
421 types. Increased weathering causes Ca loss and Ti enrichment. Both indices are a measure of
422 the geochemical maturity of soil with respect to the weathering of underlying bedrock.

423 Figure 11b displays the *aqua regia* extraction results, where again the main spread of
424 data along the Mg axis reflects the variation in Mg content between sedimentary end-member
425 (carbonate and sandstone) and mafic (ultramafic rocks) end-member parent materials. The Mg
426 loss during carbonate weathering is also marked. Increased weathering causes Ti enrichment,
427 which is less marked in the *aqua regia* extraction as compared to the XRF analytical data.
428 This is explained by the fact that Ti is not so soluble in *aqua regia*. Figure 10c, representing
429 the MMI[®] extraction results, shows a completely different pattern, where there is no Ti
430 enrichment, and Mg loss (e.g., less Mg complexation by the Mg-bearing phases like clays and
431 organic matter brought into solution by the MMI[®] extraction).



433 *Figure 11. Ca–Mg–Ti (in molecular proportions) distribution in GEMAS soil samples (black crosses),*
434 *plotted together with bedrock and Upper Continental Crust (UCC) composition (yellow circles)*
435 *according to [Parker \(1967\)](#) and [Rudnick and Gao \(2003\)](#), respectively. Grey arrowhead lines denote*
436 *compositional weathering trends of silicate and carbonate rock types towards Ca loss and Ti*
437 *enrichment. Calcium, Mg and Ti molecular proportions from (a) XRF total, (b) aqua regia extraction,*
438 *and (c) MMI[®] extraction.*

439

440 **4.4 Soil classification based on geochemical signature of parent material**

441 To classify the GEMAS soil parent materials the approach used by [Caritat et al. \(2012\)](#) was
442 applied by calculating the relative proportions of five major lithological types. According to
443 the global rock lithology model of [Amiotte Suchet et al. \(2003\)](#), the most common lithologies
444 in Europe are (1) plutonic and metamorphic, (2) shale, and (3) carbonate rocks. Based on
445 these assumption, [Caritat et al. \(2012\)](#) defined the source parent materials where plutonic and
446 metamorphic rocks (39%) and shale (37%) are dominant; carbonate rocks (14%) and sand-
447 sandstone (9.5%) are significant, whereas basalt and felsic volcanic rocks (0.5% each) play a
448 subordinate role.

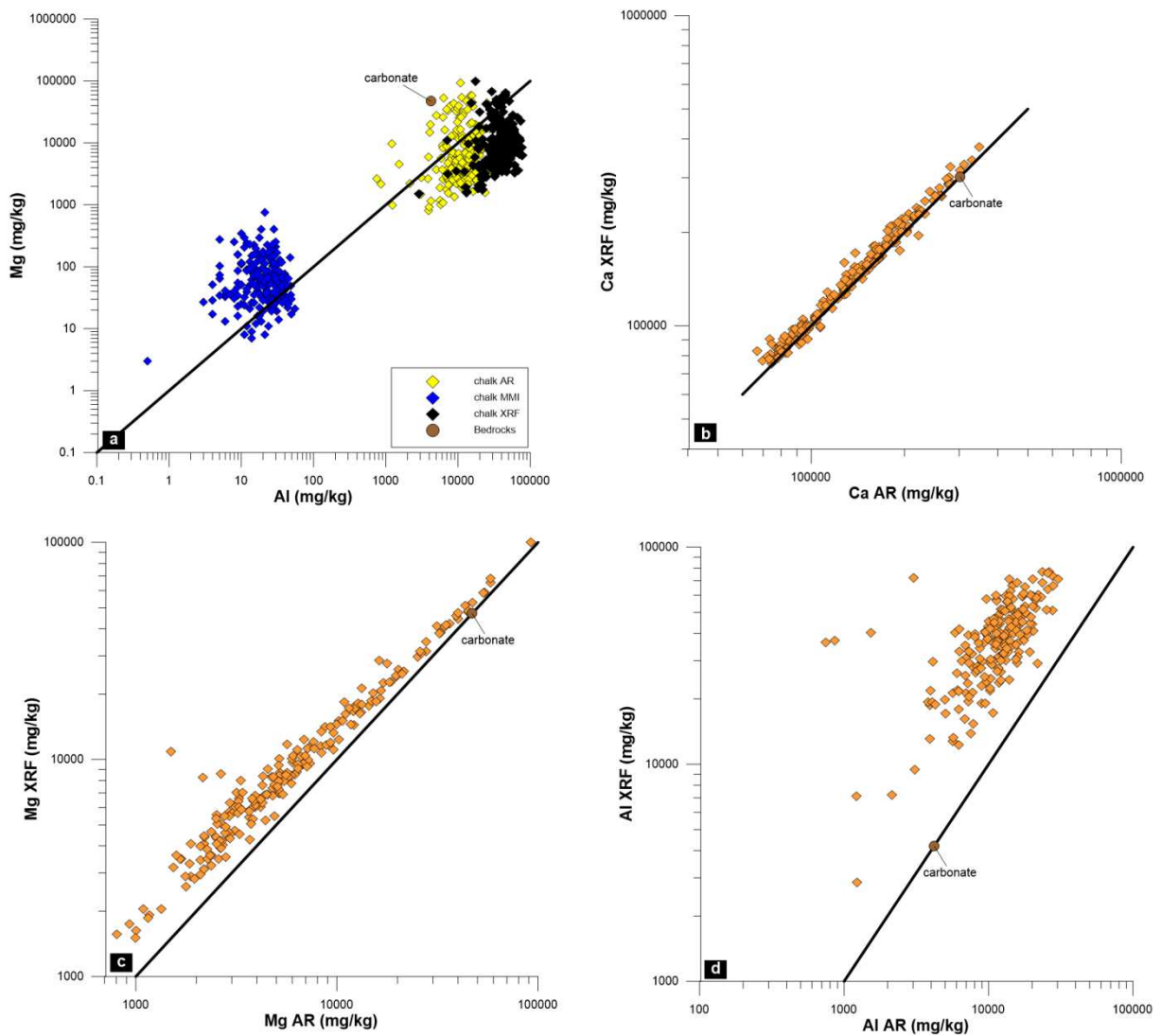
449 The Mg distribution is further depicted for chalk (carbonates) and granite, according to
450 the geological parent material subgroups constructed for processing the Ap soil results from
451 the GEMAS data set ([Birke et al., 2014b](#)). Figure 12a displays Mg and Al concentrations in
452 the geological parent material subgroup *chalk* (carbonates) for *aqua regia* and MMI[®]
453 extractions and total XRF contents. Magnesium and Al concentrations, determined by XRF
454 and *aqua regia* extraction, partly overlap and there is a clear shift on the horizontal axis for
455 the Al results reflecting major extractability difference between Mg and Al in *aqua regia*
456 digestion (55% and 22%, respectively; [Reimann et al., 2011](#)). In general, the carbonate-rich
457 soil seems to contain substantial amounts of (alumino-) silicate components, including heavy
458 minerals, which are more resistant to the *aqua regia* extraction. It is worth noting that the
459 agricultural soil samples have exclusively lower Mg and higher Al concentrations in both
460 XRF and *aqua regia* extraction results than the value of the carbonate bedrock composition

461 from [Parker \(1967\)](#), which suggests that typical carbonate-rich soil contains more clay
462 weathering products, and Mg is usually one of the elements that is depleted in such soil,
463 possibly due to leaching. The difference in Mg and Al concentrations from the *aqua regia* and
464 MMI[®] extractions is around three orders of magnitude. Further, the data from the *aqua regia*
465 extraction plot mostly below the 1:1 line, while the majority of the XRF results fall below the
466 1:1 line, and those of the MMI[®] extraction are above the 1:1 line. These observations suggest
467 that Al in carbonates, apart from its occurrence in carbonates themselves, occurs also in
468 siliceous phases and clays, and can be brought into solution by the MMI[®] extraction in the
469 chalk (carbonates) subgroup.

470 Additionally, Figures 12b to 12d show measured values by XRF compared to those
471 determined after *aqua regia* extraction for Ca, Mg and Al; in all three diagrams, the carbonate
472 bedrock composition from [Parker \(1967\)](#) is plotted. The values of Ca_{XRF} versus Ca_{AR} in
473 Figure 12b plot along the 1:1 line, with most of the values falling above it, indicating that the
474 XRF results are slightly higher than the corresponding AR. Calcium extractability is 61% for
475 all Ap soil samples, implying that extractability can be even higher for the carbonate-rich soil
476 subgroup. This excellent linear correlation also suggests that almost all Ca in this subgroup is
477 easily leachable and, therefore, hosted in minerals which can be dissolved in stronger acids
478 with high efficiency. Only a slight enrichment of the values measured by XRF over the whole
479 measured range is observed. This enrichment reflects that there is a residual fraction of Ca,
480 which cannot be extracted by the *aqua regia* extraction, mostly occurring in the silicate-clay
481 fraction.

482 The Mg_{XRF} versus Mg_{AR} values shown in Figure 12c plot parallel to the 1:1 line but
483 offset towards the XRF side and, more pronouncedly, with respect to values <10,000 mg
484 Mg/kg, i.e., lower Mg concentrations measured by XRF are clearly higher than those
485 determined by AR. The highest Mg values, measured either by XRF or AR, are close to the

486 carbonate bedrock composition from [Parker \(1967\)](#). The deviation from the 1:1 line possibly
 487 indicates that Mg-rich parent materials have more mobile Mg available than parent materials
 488 with primordial low Mg content. The marked enrichment for low Mg values, determined by
 489 XRF, suggests either a higher clay content when Mg is less concentrated, or more magnesian
 490 carbonates in accordance with lower Ca concentrations.
 491



492
 493 *Figure 12. (a) Mg versus Al content in soil subgroup 'chalk' (carbonates) obtained by XRF*
 494 *(black), aqua regia (yellow) and MMI[®] (blue) extractions; Plots comparing XRF results with*
 495 *aqua regia extraction for Ca (b), Mg (c) and Al (d) in soil subgroup 'chalk'. Reference values*
 496 *of calcareous rock together with carbonate bedrock composition are from [Parker \(1967\)](#).*
 497

498 The comparison of Al_{XRF} versus Al_{AR} values in agricultural soil (Figure 12d) shows
499 two major features. First, the concentrations measured by XRF and AR in agricultural soil are
500 higher than the Al concentration in the carbonate bedrock composition as recorded by [Parker](#)
501 ([1967](#)). This reflects the capability of AR digestion to extract Al from the clay fraction in soil.
502 Secondly, the Al concentrations lie well above the 1:1 line and mainly reflect low Al *aqua*
503 *regia* extractability in soil (ca. 20%), with the XRF data showing substantially higher values
504 than AR results. This may have implications for the weathering patterns in carbonate-rich soil
505 where Mg is the mobile and Al the residual part, resulting in Mg depletion and Al enrichment
506 in agricultural soil. This feature can be observed in karst-rich areas in the Mediterranean
507 region.

508 To evaluate the major difference between carbonate-rich and silica-rich soil parent
509 materials in relation to Mg distribution, another subgroup parent material ‘*granite*’ was
510 examined.

511 Figure 13 displays the Mg, Ca and Al concentrations in the geological parent material
512 subgroup ‘*granite*’ for *aqua regia* and MMI[®] extractions and total XRF contents. The
513 ‘*granite*’ subgroup has similar geochemical character as two other parent material subgroups:
514 Precambrian bedrock ‘*Prec*’, predominantly consisting of granitic gneiss, and ‘*schist*’
515 subgroup, which will not be discussed here in detail.

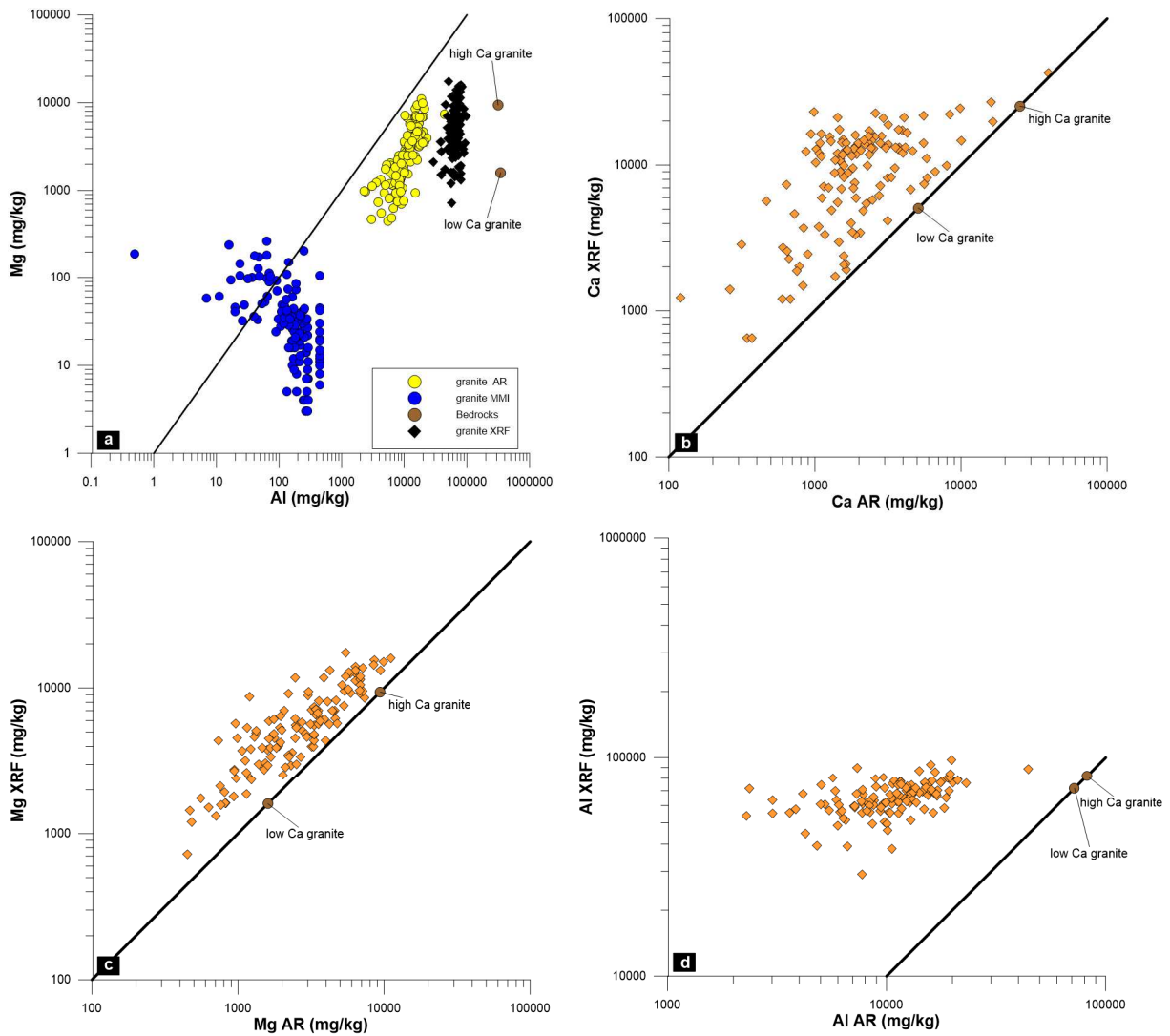
516 The major difference between the ‘*chalk*’ and ‘*granite*’ subgroups observed on the
517 plots of Mg versus Al concentrations, determined by XRF and *aqua regia* extraction, do not
518 overlap in Figure 13a. In this case, the XRF concentrations are one order of magnitude higher
519 than those measured by *aqua regia*, suggesting that Mg in agricultural soil, developed over
520 silicate parent materials, is often hosted by minerals that are insensitive to *aqua regia*
521 digestion, for example, mafic silicate minerals such as olivine, pyroxene, amphibole and some
522 micas. The refractory heavy minerals (e.g., hornblende, tourmaline, staurolite) occurring in

523 the sandy and quartz rich agricultural soil may host Mg to a minor extend, and other minerals
524 like feldspar having Mg within their structures must be considered too. Figure 13a shows that
525 there is no linear correlation between the Mg XRF and AR results. The variation in Mg
526 concentrations is much larger than Al, while the Al content is much higher in the ‘*granite*’
527 subgroup soil samples than Mg. This is an indication of the weathering status of the ‘*granite*’
528 subgroup soil, and infers a higher resistance of Al to weathering processes where a significant
529 amount of Al is held within secondary minerals like clays leading to its enrichment in this soil
530 type. While the higher mobility of Mg during weathering results in its removal from the
531 system, often in soluble form. The difference between Mg and Al concentrations from the
532 *aqua regia* and MMI[®] extractions is around three orders of magnitude. With the exception of
533 several samples plotting above the 1:1 line, reflecting a higher affinity of Mg for the hosting
534 phases (like clays and organic matter), most MMI[®] extraction results plot below the 1:1 line,
535 suggesting that the amount of organic matter is not sufficient to adsorb all Mg in the forms
536 made available by the MMI[®] extraction. It also indicates that in the part below the 1:1 line, Al
537 in the MMI[®] extraction occurs not only in siliceous phases but also in clays, which can be
538 brought into solution by the MMI[®] extraction. Thus, it is assumed that Al can be accessed by
539 living organisms via soil, plants and water, and thus it is potentially more bioavailable than
540 Mg for the parent material subgroup ‘*granite*’.

541 Figures 13b-d compare XRF total concentrations with *aqua regia* extraction results for
542 Ca, Mg and Al in the ‘*granite*’ subgroup. Comparison of Ca content in the soil subgroup
543 ‘*granite*’ (Ca_{XRF} versus Ca_{AR} , Figure 13b) shows that all samples plot above the 1:1 line, and
544 they are partly in agreement with the values of low and high Ca granite bedrock composition
545 (Parker, 1967). The higher values, measured by XRF over the whole range, indicate that Ca is
546 located in mineral phases or their interfaces, which cannot be dissolved in strong acids like
547 *aqua regia*, and mostly remain in the silicate-clay fraction. The Mg_{XRF} versus Mg_{AR} values

548 (Figure 13c) show a more confined trend than for Ca and, with the exception of some outliers,
 549 are partly in agreement with the concentration range for granite bedrock composition from
 550 [Parker \(1967\)](#). The higher values, measured by XRF over the whole range, reflect the non-
 551 extractable Mg remaining in the silicate-clay fraction. The plot of Al_{XRF} versus Al_{AR} values
 552 (Figure 13d) is extremely controlled by low Al extractability, and XRF results are tenfold
 553 higher than the corresponding AR. Considering that feldspar is the most common Al host in
 554 soil developed on crystalline and felsic bedrocks, and it is difficult to dissolve in strong acids,
 555 the Al from AR originates most likely from more advanced weathering products such as
 556 clays.

557

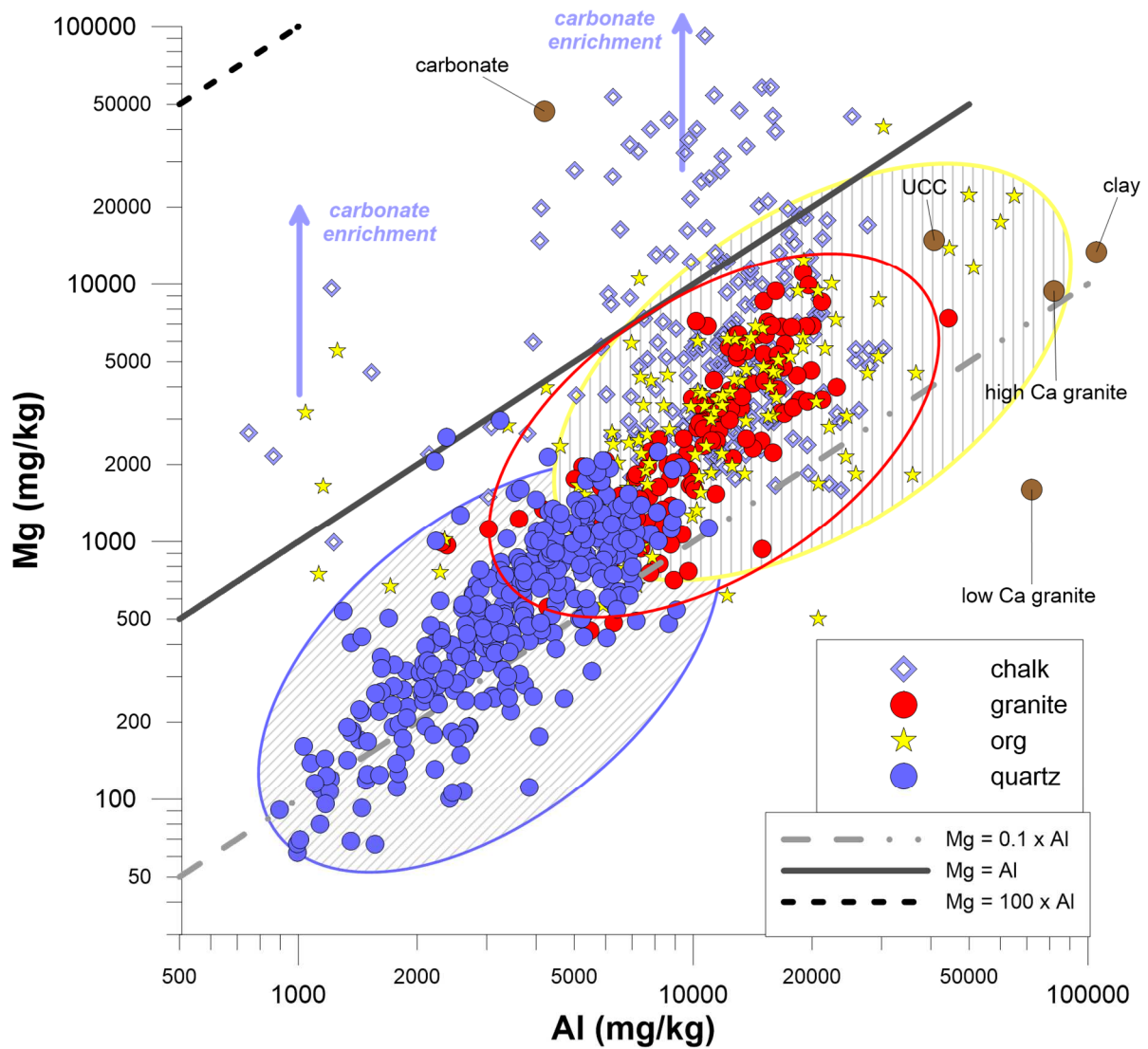


558

559 *Figure 13. (a) Mg versus Al content in the soil subgroup 'granite' obtained by XRF (black),*
560 *aqua regia (yellow) and MMI[®] (blue) extractions. Plots comparing XRF results with aqua*
561 *regia extraction for Ca (b), Mg (c) and Al (d) in the soil subgroup 'granite'. Reference values*
562 *of high and low Ca granite bedrock composition are from Parker (1967).*
563

564 The solid phases commonly anticipated to dissolve, during sequential extraction,
565 according to the initial work of Tessier et al. (1979), are carbonates (exchangeable ions and
566 acid extractable), Fe–Mn-hydroxides (reducible), sulphides and organic matter (oxidisable).
567 The other phases, e.g., some silicates and well-crystallised oxides, are generally not extracted
568 by *aqua regia* (residual). Such sequential extraction is used for prediction of deficiency or
569 toxicity and assessment of soil trace element status in soil (Ure, 1996). The AR digestion has
570 the capability to extract elements from the clay fraction, as well as to dissolve Fe-Mn oxides
571 and carbonates and organic matter and is considered to assess the extent of element
572 concentration in a pseudo-total digestion (Ure, 1996). Strong acid digestions, such as *aqua*
573 *regia*, are commonly employed even though silicates and other refractory oxides are not
574 completely dissolved, the recovery is often >75% and never 100% (Chen and Ma, 2001).

575 Clay minerals may contain appreciable quantities of Mg either in inter lattice sites or
576 in exchange positions resulting from broken edges or unbalanced charges. Magnesium, like
577 Al, is especially common in montmorillonite, chlorites, and vermiculites (Kahle, 1965).
578 However, Al interlayers in soil, developed from silicate bedrocks (granite, gneiss and schist),
579 are more pronounced and stable than in soil derived from basaltic rock or limestone
580 (Sawhney, 1960). Mixed Mg-Al hydroxides occur frequently (Brown and Gastuche, 1967;
581 Mascolo and Marino, 1980), and both clay minerals and Al or Fe oxides/hydroxides can sorb
582 dissolved organic carbon (DOC). Surfaces of minerals in soil, capable of sorbing DOC, may
583 be distinguished into two dominant types: (1) surfaces of phyllosilicate clay minerals
584 containing cation exchange sites, and (2) surfaces on the external periphery of pedogenic
585 oxides/oxyhydroxides minerals (Kahle et al., 2004), with oxides usually being better sorbents
586 than phyllosilicate clay minerals (Jardine et al., 1989; Kaiser and Zech, 2000).



587

588 *Figure 14. Plot of Mg vs. Al contents in Ap soil samples for aqua regia extraction data for the*
 589 *parent material subgroups ‘chalk’, ‘granite’, ‘org’ (organic soil), and ‘quartz’ (soil*
 590 *developed on coarse-grained sandy deposits). The blue shaded field delineates quartz parent*
 591 *material group; the yellow shaded area – the organic parent material soil group, and the red*
 592 *ellipsoid – the granite parent material group.*
 593

594 In Figure 14, the aqua regia Mg vs. Al concentrations in Ap soil samples were used for
 595 the four parent material subgroups ‘chalk’ (carbonates), ‘granite’, organic soil subgroup (org)
 596 and ‘quartz’ (soil developed on coarse-grained sandy deposits). The first two subgroups
 597 (‘chalk’ and ‘granite’) can help to investigate the role of organic residues in terms of sorption
 598 with the subgroup organic soil (org), and the same role of clay minerals regarding soil

599 developed on coarse-grained sandy deposits, e.g., the moraines of the last glaciation, with the
600 subgroup ‘*quartz*’ (Négrel et al., 2018a).

601 The *aqua regia* extraction results for the subgroups organic soil (*org*) and soil
602 developed on coarse-grained sandy deposits (*quartz*) plot below the Mg/Al 1:1 line, and
603 mostly above the 0.1 Mg/Al line. Both are marked by the hatched ellipses that, with the
604 exception of some outliers, encompass the majority of data. An enrichment of the Mg/Al ratio
605 for ‘*quartz*’ can be observed together with enrichment for the highest Mg and Al
606 concentrations. For organic soil (*org*), the data of the *aqua regia* extraction show higher
607 concentration for Mg and Al in comparison to the range of subgroup ‘*quartz*’, and an overlap
608 of the lower concentrations of the subgroup ‘*org*’ with the higher values of subgroup ‘*quartz*’.
609 The range observed in the ‘*granite*’ subgroup in Figure 14, has similar Mg and Al
610 concentrations as most of the ‘*organic*’ soil samples, with the exception of some outliers. As
611 far as the role of organic residues in the ‘*granite*’ subgroup, this can be interpreted as the
612 presence of Mg-Al rich mineral phases, most likely Al or Fe oxides/hydroxides. For the
613 ‘*granite*’ subgroup, the importance of clay minerals and fine-grained hydroxides in the
614 geochemical cycles of Mg and Al in soil start from the clay end-member from Parker (1967),
615 and follow a downward trend along the Mg/Al 0.1 ratio line towards the lowermost values of
616 Mg and Al observed in the ‘*quartz*’ subgroup. The role of clay minerals, thus, appears not so
617 important compared to that played by the organic residues in the ‘*granite*’ subgroup, as the
618 highest Mg-Al concentrations for the ‘*quartz*’ subgroup overlap with the lowest
619 concentrations observed in the ‘*granite*’ subgroup.

620

621 **5 – Conclusions**

622

623 The GEMAS European agricultural soil results can be used to define the ‘normal’ Mg
624 concentration ranges (25th to 75th percentile of the distribution) in agricultural soil at the
625 European scale using three different analytical techniques. Normal total Mg concentrations
626 (XRF) range from 3015 - 9407 mg/kg. In an *aqua regia* extraction, they range from 1370 -
627 5447 mg/kg Mg. For the MMI[®] extraction, which comes closest to ‘plant available’ contents,
628 the normal range is from 26 to 103 mg/kg Mg.

629 Due to the importance of Mg for plants, the occurrence of unusually low
630 concentrations in agricultural soil is of more concern than the high concentration range. In
631 Europe, unusually low Mg concentrations in agricultural soil for both XRF and *aqua regia*
632 results are observed on top of the quartz-rich glacial sediments in north-central Europe
633 (Poland, Baltic States, N. Germany), and a sandstone unit at the Swedish/Norwegian border.
634 In contrast, unusually high Mg concentrations occur predominantly on top of known ophiolite
635 belts and carbonates (e.g., Hellas and eastern Spain, respectively). The maximum extent of the
636 last glaciation is visible on all three maps as a clear Mg concentration break. In the MMI[®]
637 extraction, a quite different pattern emerges. Large areas in Fennoscandia additionally show
638 low Mg concentrations, indicating that weathering and soil formation are still in a stage where
639 many Mg-bearing minerals are not easily dissolved. High concentrations in MMI[®] do still
640 predominantly occur on top of ophiolites, however, on a much more restricted scale than
641 observed for *aqua regia* available or total XRF concentrations. Thus, geology still plays the
642 key role in determining the distribution of Mg in agricultural soil at the European scale, while
643 agricultural practice and the use of fertilisers seem to play a subordinate role.

644 To better understand the factors that determine the availability of Mg, the *aqua regia*
645 and MMI[®] extraction results were studied in more detail on four different substrates (organic
646 soil, quartz-rich soil, soil developed on granite and soil on top of calcareous rocks). The

647 results highlight the importance of organic material, the presence of clay minerals (grain size
648 distribution of soil) and fine-grained hydroxides for the observed element concentrations.

649 **Acknowledgements**

650
651 The GEMAS project is a cooperative project of the EuroGeoSurveys Geochemistry Expert Group with
652 a number of outside organisations (e.g., Alterra, The Netherlands; Norwegian Forest and Landscape
653 Institute; Research Group Swiss Soil Monitoring Network, Swiss Research Station Agroscope
654 Reckenholz-Tänikon, several Ministries of the Environment and University Departments of
655 Geosciences, Chemistry and Mathematics in a number of European countries and New Zealand;
656 ARCHE Consulting in Belgium; CSIRO Land and Water in Adelaide, Australia). The analytical work
657 was co-financed by the following industry organisations: Eurometaux, European Borates Association,
658 European Copper Institute, European Precious Metals Federation, International Antimony Association,
659 International Lead Association-Europe, International Manganese Institute, International Molybdenum
660 Association, International Tin Research Institute, International Zinc Association, The Cobalt
661 Development Institute, The Nickel Institute, The (REACH) Selenium and Tellurium Consortium and
662 The (REACH) Vanadium Consortium. The Directors of the European Geological Surveys, and the
663 additional participating organisations, are thanked for making sampling of almost all of Europe in a
664 tight time schedule possible. The Federal Institute for Geosciences and Natural Resources (BGR), the
665 Geological Survey of Norway and SGS (Canada) are thanked for special analytical input to the
666 project.

667

668 **References**

669 Aatos, S., Tarvainen, T., Räisänen, M.L., Salminen, R., 1994. Method for determining the normative
670 mineralogy of the fine fraction of till. *Geologi* 46, 39-42.
671 Albanese, S., Sadeghi, M., Lima, A., Cicchella, D., Dinelli, E., Valera, P., Falconi, M., Demetriades,
672 A., De Vivo, B., The GEMAS Project Team, 2015. GEMAS: chromium, Ni, Co and Cu in
673 agricultural and grazing land soil of Europe. *J. Geochem. Explor.* 154, 81-93.

674 Amiotte Suchet, P., Probst, J.-L., Ludwig, W., 2003. Worldwide distribution of continental rock
675 lithology: implications for the atmospheric/soil CO₂ uptake by continental weathering and
676 alkalinity river transport to the oceans. *Glob. Biogeochem. Cycles* 17, 1038-1051.

677 [Aitchison, J., 1986.](#) The statistical analysis of compositional data. London: Chapman & Hall, 416 pp.

678 Beus, A.A., Grigorian, S.V., 1977. Geochemistry exploration methods for mineral deposit. Applied
679 Publishing House, Wilmette, Illinois, 277 pp.

680 Birke, M., Reimann, C., Karl Fabian, K., 2014a. Analytical Methods Used in the GEMAS Project.
681 Chapter 5 In: C. Reimann, M. Birke, A. Demetriades, P. Filzmoser, P. O'Connor (Editors),
682 Chemistry of Europe's agricultural soils – Part A: Methodology and interpretation of the GEMAS
683 data set. *Geologisches Jahrbuch (Reihe B102)*, Schweizerbarth, Hannover, 41-46.

684 Birke, M., Rauch, U., Reimann, C., 2014b. Supporting Information for Interpretation of Geochemical
685 Maps. Chapter 10 In: C. Reimann, M. Birke, A. Demetriades, P. Filzmoser, P. O'Connor (Editors),
686 Chemistry of Europe's agricultural soils – Part A: Methodology and interpretation of the GEMAS
687 data set. *Geologisches Jahrbuch (Reihe B102)*, Schweizerbarth, Hannover, 93-102.

688 Birke, M., Reimann, R., Oorts, K., Rauch, U., Demetriades, A., Dinelli, E., Ladenberger, A., Halamić,
689 J. Gosar, M., Jähne-Klingberg, F., the GEMAS Project Team, 2016. Use of GEMAS data for risk
690 assessment of cadmium in European agricultural and grazing land soil under the REACH
691 Regulation. *App. Geochem.* 74, 109–121.

692 Birke, M., Reimann, C., Rauch, U., Ladenberger, A., Demetriades, A., Jähne-Klingberg, F., Oorts, K.,
693 Gosar, M., Dinelli, E., Halamić, J., the GEMAS Project Team, 2017. GEMAS: Cadmium
694 distribution and its sources in agricultural and grazing land soil of Europe — Original data versus
695 clr-transformed data. *J. Geochem Explor.* 173, 13-30.

696 Brown, G., Gastuche, M.C., 1967. Mixed Magnesium-Aluminium hydroxides. II. Structure and
697 structural chemistry of synthetic hydroxycarbonates and related minerals and compounds. *Clay*
698 *Minerals*, 7(2), 193-201.

699 Buccianti, A., Pawlowsky-Glahn, V., Mateu-Figueras, G. (editors), 2006. Compositional data analysis
700 in the geosciences: from theory to practice. London: Geological Society, 224 pp.

701 Caritat de, P., Reimann, C., the NGSA Team, GEMAS team, 2012. Comparing results from two
702 continental geochemical surveys to world soil composition and deriving Predicted Empirical
703 Global Soil (PEGS2) reference values. *Earth Planet. Sci. Lett.* 319–320, 269–276.

704 Cassard, D., Bertrand, G., Maldan, F., Gaàl, G., Kaija, J., Aatos, S., Angel, J.M., Arvanitidis, N.,
705 Ballas, D., Billa, M., Christidis, C., Dimitrova, D., Eilu, P., Filipe, A., Gazea, E., Inverno, C.,
706 Kauniskangas, E., Maki, T., Matos, J., Meliani, M., Michael, C., Mladenova, V., Navas, J.,
707 Niedbal, M., Perantonis, G., Pyra, J., Santana, H., Serafimovski, T., Serrano, J.J., Strengell, J.,
708 Tasev, G., Tornos, F., Tudor, G., 2012. ProMine pan-European mineral deposit database: a new
709 dataset for assessing primary mineral resources in Europe. Workshop on: Mineral Resources

710 Potential Maps: A Tool for Discovering Future Deposits. 12th–14th March 2012, Nancy, France,
711 Proceedings, pp. 9–13.

712 Cassard, D., Bertrand, G., Billa, M., Serrano, J.J., Tourliere, B., Angel, J.M., Gaal, G., 2015. ProMine
713 mineral databases: new tools to assess primary and secondary mineral resources in Europe (Chapter
714 2). In: Weihed, P. (Ed.), 3D, 4D and Predictive Modelling of Major Mineral Belts in Europe.
715 Mineral Resource Reviews. Springer International Publishing, pp. 9–58.
716 https://doi.org/10.1007/978-3-319-17428-0_2.

717 Chen, M., Ma, L.Q., 2001. Comparison of three *aqua regia* digestion methods for twenty Florida soils.
718 Soil Sci. Soc. Amer. J., 65, 491-499.

719 Christie, T., Brathwaite, B., 2008. Mineral Commodity Report 19 - Beryllium, Gallium, Lithium,
720 Magnesium, Uranium and Zirconium. Institute of Geological and Nuclear Sciences Ltd, New
721 Zealand, 16 pp. [https://www.nzpam.govt.nz/assets/Uploads/doing-business/mineral-](https://www.nzpam.govt.nz/assets/Uploads/doing-business/mineral-potential/beryllium.pdf)
722 [potential/beryllium.pdf](https://www.nzpam.govt.nz/assets/Uploads/doing-business/mineral-potential/beryllium.pdf).

723 Demetriades, A., 2011. Understanding the quality of chemical data from the urban environment – Part
724 2: Measurement uncertainty in the decision-making process. Chapter 6, In: C.C. Johnson, A.
725 Demetriades, J. Locutura, R.T. Ottesen (Editors), Mapping the chemical environment of urban
726 areas. Wiley-Blackwell, John Wiley & Sons Ltd., Chichester, West Sussex, U.K., 77-98;
727 <https://doi.org/10.1002/9780470670071.ch6>.

728 Demetriades, A., Reimann, C., 2014. Mineral deposits in Europe. Chapter 3 In: C. Reimann, M. Birke,
729 A. Demetriades, P. Filzmoser, P. O'Connor (Editors), Chemistry of Europe's agricultural soils –
730 Part B: General background information and further analysis of the GEMAS data set. Geologisches
731 Jahrbuch (Reihe B103), Schweizerbarth, Hannover, 71-78.

732 Demetriades, A., Reimann, C., Filzmoser, P., 2014. Evaluation of GEMAS project quality control
733 results. Chapter 6 In: C. Reimann, M. Birke, A. Demetriades, P. Filzmoser, P. O'Connor (Editors),
734 Chemistry of Europe's agricultural soils – Part A: Methodology and interpretation of the GEMAS
735 data set Geologisches Jahrbuch (Reihe B102), Schweizerbarth, Hannover, 47-60.

736 Dolezal, J., Povondra, C., Sulcek, Z., 1968. Decomposition Techniques in Inorganic Analysis. Iliffe,
737 London, 224 pp.

738 European Commission, 2017. Study on the review of the list of Critical Raw Materials: Criticality
739 assessments. Brussels, 13.9.2017, COM (2017) 490 final, 92 pp.

740 Fabian, C., Reimann, C., Fabian, K., Birke, M., Baritz, R., Haslinger, E., The GEMAS Project Team,
741 2014. GEMAS: Spatial distribution of the pH of European agricultural and grazing land soil. App.
742 Geochem. 48, 207-216.

743 Filzmoser, P., Reimann, C., Birke, M., 2014. Univariate Data Analysis and Mapping. Chapter 8 In: C.
744 Reimann, M. Birke, A. Demetriades, P. Filzmoser, P. O'Connor (Editors), Chemistry of Europe's
745 agricultural soils – Part A: Methodology and interpretation of the GEMAS data set. Geologisches
746 Jahrbuch (Reihe B102), Schweizerbarth, Hannover, 67-81.

747 Günther, A., Reichenbach, P., Malet, J.-P., Van Den Eeckhaut, M., Hervás, J., Dashwood, C.,
748 Guzzetti, F., 2013. Tier-based approaches for landslide susceptibility assessment in Europe
749 Landslides 10, 529-546.

750 Hoogewerff, J.A., Reimann, C., Ueckermann, H., Frei, R., Frei, K.M., van Aswegen, Th., Stirling, C.,
751 Reid, M., Clayton, A., Ladenberger, A., The GEMAS Project Team, 2019. Bioavailable $^{87}\text{Sr}/^{86}\text{Sr}$
752 in European soils: A baseline for provenancing studies. *Sci. Tot. Env.* 672, 1033-1044.
753 <https://doi.org/10.1016/j.scitotenv.2019.03.387>.

754 Jardine, P.M., Weber, N.L., McCarthy, J.F., 1989. Mechanisms of dissolved organic carbon adsorption
755 on soil. *Soil Sci. Soc. Amer. J.* 53, 1378–1385.

756 Jordan, G., Petrik, A., De Vivo, B., Albanese, S., Demetriades, A., Sadeghi, M., The GEMAS Project
757 Team, 2018. GEMAS: Spatial analysis of the Ni distribution on a continental-scale using digital
758 image processing techniques on European agricultural soil data. *J. Geochem. Explor.*, 186, 143-
759 157; <https://doi.org/10.1016/j.gexplo.2017.11.011>.

760 Kahle, C.F., 1965. Possible roles of clay minerals in the formation of dolomite. *Jour. Sed.* 448-453.

761 Kahle, M., Kleber, M., Jahn, R., 2004. Retention of dissolved organic matter by phyllosilicate and soil
762 clay fractions in relation to mineral properties. *Org. Geochem.*, 35(3), 269-276.

763 Kaiser, K., Zech, W., 1997. Competitive sorption of dissolved organic matter fractions to soils and
764 related mineral phases. *Soil Sci. Soc. Amer. J.* 61, 64–69.

765 Kasanzu, C., Maboko, M.A.H., Manya, S., 2008. Geochemistry of fine-grained clastic sedimentary
766 rocks of the Neoproterozoic Ikorongo Group, NE Tanzania: Implications for provenance and
767 source rock weathering. *Prec. Res.*, 164, 201–213.

768 Ladenberger, A., Demetriades, A., Reimann, C., Birke, M., Sadeghi, M., Uhlback, J., Andersson, M.,
769 Jonsson, E., the GEMAS Project Team, 2015. GEMAS: Indium in agricultural and grazing land
770 soil of Europe e its source and geochemical distribution patterns. *J. Geochem. Explor.* 154, 61-80.

771 [Mackovych, D., Lucivjansky, P., 2014. Preparation of GEMAS project samples and standards. In:](#)
772 [Reimann, C., Birke, M., Demetriades, A., Filzmoser, P., O'Connor, P. \(eds.\), 2014. Chemistry of](#)
773 [Europe's agricultural soils – Part A: Methodology and interpretation of the GEMAS dataset.](#)
774 [Geologisches Jahrbuch \(Reihe B\), Schweizerbarth, Stuttgart, 37-40.](#)

775 Mann, A., Reimann, C., Caritat, P. de, Turner, N., Birke, M., the GEMAS Project Team, 2015. Mobile
776 Metal Ion[®] analysis of European agricultural soils: bioavailability, weathering, geogenic patterns
777 and anthropogenic anomalies. *Geochem. Expl. Env. Anal.* 15, 99-112.

778 Mann, A.M., 2010. Strong versus weak digestions: ligand-based soil extraction geochemistry.
779 *Geochem. Expl. Env. Anal.* 10, 17-26.

780 Mann, A.M., Birrell, R.D., Mann, A.T., Humphreys, B., Perdrix, G.L., 1998. Application of the
781 mobile metal ion technique to routine geochemical exploration. *J. Geochem. Explor.* 61, 7-102.

782 Mann, A., Reimann, C., De Caritat, P., Turner, N., Birke, M., the GEMAS Project Team, 2014a.
783 Mobile Metal Ion[®] analysis of European agricultural soils: bioavailability, weathering, geogenic
784 patterns and anthropogenic anomalies. *Geochem. Expl. Env. Anal.* 15, 99–112.

785 Mann, A., Reimann, C., De Caritat, P., Turner, N., 2014b. Mobile metal ion analysis of European
786 agricultural soil. In: Reimann, C., Birke, M., Demetriades, A., Filmoser, P., O'Connor, P. (Eds.),
787 Chemistry of Europe's Agricultural Soil, *Geologisches Jahrbuch B*, 203-231.

788 Mascolo, G., Marino, O., 1980. A new synthesis and characterization of magnesium-aluminium
789 hydroxides 1. *Mineral. Mag.*, 43(329), 619-621.

790 Matschullat, J., Reimann, C., Birke, M., Santos Carvalho, D. dos, the GEMAS Project Team, 2018.
791 GEMAS: CNS concentrations and C/N ratios in European agricultural soil. *Sci. Total Environ* 627,
792 975-984.

793 Négrel, Ph., Sadeghi, M., Ladenberger, A., Reimann, C., Birke, M., the GEMAS Project Team, 2015.
794 Geochemical fingerprinting and source discrimination of agricultural soils at continental scale.
795 *Chem. Geol.* 396, 1-15.

796 Négrel, Ph., Ladenberger, A., Reimann, C., Birke, M., Sadeghi, M., the GEMAS Project Team, 2016.
797 GEMAS: source, distribution patterns and geochemical behavior of Ge in agricultural and grazing
798 land soils at European continental scale. *App. Geochem.* 72, 113-124.

799 Négrel, Ph., Cicchella, D., Albanese, S., de Vivo, B., Reimann, C., Ladenberger, A., Birke, M., De
800 Vos, W., Dinelli, E., Lima, A.M., O'Connor, P.J., Salpeteur, I., Tarvainen, T., the GEMAS Project
801 Team, 2018a. U-Th signatures of land soils at European continental scale (GEMAS): distribution,
802 weathering patterns and processes controlling their concentrations. *Sci. Total Environ.* 622–623,
803 1277-1293.

804 Négrel, Ph., Ladenberger, A., Reimann, C., Birke, M., Sadeghi, M., the GEMAS Project Team, 2018b.
805 Distribution of Rb, Ga and Cs in agricultural land soils at European continental scale (GEMAS):
806 Implications for weathering conditions and provenance. *Chem. Geol.* 479, 188-203.

807 Négrel, Ph., Ladenberger, A., Reimann, C., Birke, M., Demetriades, A., Sadeghi, M., the GEMAS
808 Project Team, 2019. GEMAS: Geochemical background and mineral potential of emerging tech-
809 critical elements in Europe revealed from low-sampling density geochemical mapping. *App.*
810 *Geochem.* 111, 104425.

811 Niskavaara, H., Reimann, C., Chekushin, V., Kashulina, G., 1997. Seasonal variability of total and
812 easily leachable element contents in topsoils (0-5 cm) from eight catchments in the European
813 Arctic (Finland, Norway and Russia). *Environmental Pollution*, 96(2), 261-274;
814 [https://doi.org/10.1016/S0269-7491\(97\)00031-6](https://doi.org/10.1016/S0269-7491(97)00031-6).

815 Ottesen, R.T., Birke, M., Finne, T.E., Gosar, M., Locutura, J., Reimann, C., Tarvainen, T., the
816 GEMAS team, 2013. Mercury in European agricultural and grazing land soils. *App. Geochem.* 33,
817 1-12.

818 Pawlowsky-Glahn, V., Buccianti, A., 2011. Compositional data analysis: theory and applications.
819 Chichester: Wiley, 378 pp.

820 Parker, R.L., 1967. Composition of the Earth's crust. U.S. Geological Survey Professional Paper 440-
821 D, 17 pp.

822 Pohl, W.L., 1990. Genesis of magnesite deposits – models and trends. *Geologische Rundschau* 79,
823 291-299. <https://doi.org/10.1007/BF01830626>

824 Räsänen, M.L., Tenhola, M., Mäkinen, J., 1992. Relationship between mineralogy and physico-
825 chemical properties of till in central Finland. *Bull. Geol. Soc. Finland* 64, 35-58.

826 REACH., 2006. Regulation (EC) No 1907/2006 of the European Parliament and of the Council of 18
827 December 2006 concerning the Registration, Evaluation, Authorisation and Restriction of
828 Chemicals (REACH), establishing a European Chemicals Agency, <http://eur-lex.europa.eu/eli/reg/2006/1907/oj>.

830 Reimann, C., Kriete, C., 2014. Trueness of GEMAS Analytical Results - the Ring Test. Chapter 7 In:
831 C. Reimann, M. Birke, A. Demetriades, P. Filzmoser & P. O'Connor (Editors), *Chemistry of
832 Europe's agricultural soils – Part A: Methodology and interpretation of the GEMAS data set.*
833 *Geologisches Jahrbuch (Reihe B102)*, Schweizerbarth, Hannover, 61-65.

834 Reimann, C., Demetriades, A., Eggen, O.A., Filzmoser, P. and EuroGeoSurveys Geochemistry
835 Working Group, 2009. The EuroGeoSurveys geochemical mapping of agricultural and grazing land
836 soils project (GEMAS) - Evaluation of quality control results of *aqua regia* extraction analysis.
837 NGU Report 2009.049. Geological Survey of Norway, Trondheim, 94 pp.
838 http://www.ngu.no/upload/publikasjoner/rapporter/2009/2009_049.pdf.

839 Reimann, C., Demetriades, A., Eggen, O.A., Filzmoser, P. and EuroGeoSurveys Geochemistry
840 Working Group, 2011. The EuroGeoSurveys geochemical mapping of agricultural and grazing land
841 soils project (GEMAS) – Evaluation of quality control results of total C and S, total organic carbon
842 (TOC), cation exchange capacity (CEC), XRF, pH, and particle size distribution (PSD) analysis.
843 NGU Report 2011.043. Geological Survey of Norway, Trondheim, 92 pp.
844 http://www.ngu.no/upload/publikasjoner/rapporter/2011/2011_043.pdf.

845 Reimann, C., Flem, B., Fabian, K., Birke, M., Ladenberger, A., Négrel, Ph., Hoogewerff, J., 2012a.
846 Lead and lead isotopes in agricultural soils of Europe - the continental perspective. *App. Geochem.*,
847 27, 532–542.

848 Reimann, C., Demetriades, A., Birke, M., Eggen, O. A., Filzmoser, P., Kriete, C., EuroGeoSurveys
849 Geochemistry Expert Group, 2012b. The EuroGeoSurveys Geochemical Mapping of Agricultural
850 and grazing land Soils project (GEMAS) – Evaluation of quality control results of particle size
851 estimation by MIR prediction, Pb-isotope and MMI[®] extraction analyses and results of the GEMAS
852 ring test for the standards Ap and Gr. NGU Report 2012.051, 136 pp.,
853 http://www.ngu.no/upload/Publikasjoner/Rapporter/2012/2012_051.

854 Reimann, C., Caritat, P. de, GEMAS team, NGS team, 2012c. New soil composition data for Europe
855 and Australia: demonstrating comparability, identifying continental-scale processes and learning
856 lessons for global geochemical mapping. *Sci. Total Environ.* 416, 239-252.

857 Reimann, C., Birke, M., Demetriades, A., Filzmoser, P., O'Connor, P. (eds.), 2014a. Chemistry of
858 Europe's agricultural soils – Part A: Methodology and interpretation of the GEMAS dataset.
859 *Geologisches Jahrbuch (Reihe B)*, Schweizerbarth, Stuttgart, 528 pp.

860 Reimann, C., Birke, M., Demetriades, A., Filzmoser, P., O'Connor, P. (eds.), 2014b. Chemistry of
861 Europe's agricultural soils – Part B: General background information and further analysis of the
862 GEMAS dataset. *Geologisches Jahrbuch (Reihe B)*, Schweizerbarth, Stuttgart, 352 pp.

863 Reimann, C., Demetriades, A., Birke, M., Filzmoser P., O'Connor, P., Halamić, J., Ladenberger, A.,
864 the GEMAS Project Team, 2014c. Distribution of elements/ parameters in agricultural and grazing
865 land soil of Europe. Chapter 11 In: C. Reimann, M. Birke, A. Demetriades, P. Filzmoser & P.
866 O'Connor (Editors), Chemistry of Europe's agricultural soils – Part A: Methodology and
867 interpretation of the GEMAS data set. *Geologisches Jahrbuch (Reihe B102)*, Schweizerbarth,
868 Hannover, 103-474.

869 Rudnick, R.L., Gao, S., 2003. Composition of the continental crust. In: Holland, H.D., Turekian, K.K.,
870 Rudnick, R.L. (Eds.), *Treatise on Geochemistry, The Crust*, vol. 3, Elsevier-Pergamon, Oxford, 1-
871 64.

872 Sadeghi, M., Petrosino, P., Ladenberger, A., Albanese, S., Andersson, M., Morris, G., Lima, A.M., De
873 Vivo, B., the GEMAS team, 2013. Ce, La and Y concentrations in agricultural and grazing-land
874 soils of Europe. *J. Geochem. Explor.* 133, 202-213.

875 Sadeghi, M., Albanese, S., Morris, G., Ladenberger, A., Andersson, M., Cannatelli, C., Lima, A., De
876 Vivo, B., 2015. REE concentrations in agricultural soil in Sweden and Italy: Comparison of weak
877 MMI® extraction with near total extraction data. *App. Geochem.* 63, 22-36.

878 Sastre, J., Sahuquillo, A., Vidal, M., Rauret, G., 2002. Determination of Cd, Cu, Pb and Zn in
879 environmental samples: microwave-assisted total digestion versus aqua regia and nitric acid
880 extraction. *Analytica Chimica Acta*, 462(1), 59-72; [https://doi.org/10.1016/S0003-2670\(02\)00307-](https://doi.org/10.1016/S0003-2670(02)00307-0)
881 0.

882 Santos, S.N. dos, Alleoni, L.R.F., 2013. Methods for Extracting Heavy Metals in Soils from the
883 Southwestern Amazon, Brazil. *Water Air Soil Pollut* 224, 1430. [https://doi.org/10.1007/s11270-](https://doi.org/10.1007/s11270-012-1430-z)
884 012-1430-z.

885 Scheib, A.J., Flight, D.M.A., Birke, M., Tarvainen, T., Locutura, J., GEMAS Project Team, 2012. The
886 geochemistry of niobium and its distribution and relative mobility in agricultural soils of Europe.
887 *Geochem. Explor. Environ. Anal.* 12, 293-302.

888 Scheib, A.J., Birke, M., Dinelli, E., GEMAS Project Team, 2014. Geochemical evidence of aeolian
889 deposits in European soils. *Boreas* 43(1), 175-192. <https://doi.org/10.1111/bor.12029>.

890 Sawhney, B.L., 1960. Aluminium interlayers in clay minerals. Transactions 7th Int. Congr. Soil Sci. 4,
891 476-481.

892 Snäll, S., Liljefors, T., 2000. Leachability of major elements from minerals in strong acids. J.
893 Geochem. Explor. 71(1), 1-12.

894 Tarvainen, T., Albanese, S., Birke, M., Ponavic, M., Reimann, C., the GEMAS Team, 2013. Arsenic
895 in agricultural and grazing land soils of Europe. App. Geochem. 28, 2-10.

896 Tessier, A., Campbell, P.G.C., Bisson, M., 1979. Sequential extraction procedure for the speciation of
897 particulate trace metals. Anal. Chem. 51, 844–851.

898 Ure, A.M., 1996. Single extraction schemes for soil analysis and related applications. Sci. Total
899 Environ, 178, 3-10.

900 Vercoutere, K., Fortunati, U., Muntau, H., Griepink, B., Maier, E.A., 1995. The certified reference
901 materials CRM 142 R light sandy soil, CRM 143 R sewage sludge amended soil and CRM145 R
902 sewage sludge for quality control in monitoring environmental and soil pollution. Fresenius'
903 Journal of Analytical Chemistry, 352, 197–202; <https://doi.org/10.1007/BF00322326>. Vilà, M.,
904 Martínez-Lladó, X. 2015. Approaching earth surface geochemical variability from representative
905 samples of geological units: The Congost River basin case study. J. Geochem. Explor. 148, 79–95.

906 Xu, H., Demetriades, A., Reimann, C., Jiménez, J.J., Filser, J., Zhang, C., GEMAS Project, Team,
907 2019. Identification of the co-existence of low total organic carbon contents and low pH values in
908 agricultural soil in north-central Europe using hot spot analysis based on GEMAS project data.
909 Science of the Total Environment 678, 94-104. <https://doi.org/10.1016/j.scitotenv.2019.04.382>.

910 Zeeberg, J. J., 1998. The European sand belt in Eastern Europe – and comparison of Late Glacial dune
911 orientation with GCM simulation results. Boreas 27, 127–139.